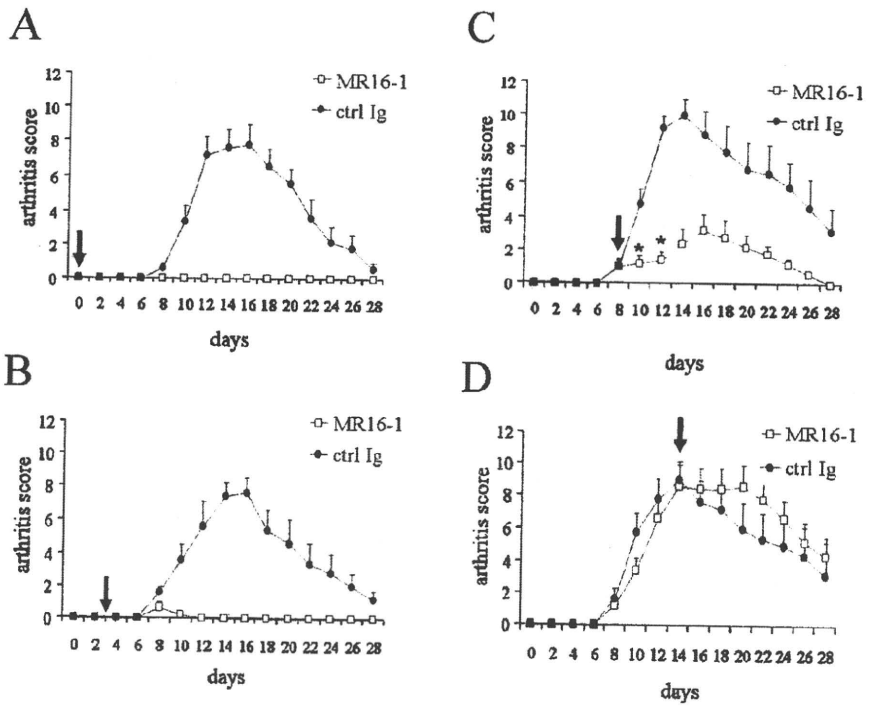

Figure 4. Inhibition of the development of arthritis by treatment with anti–interleukin-6 receptor (anti–IL-6R) monoclonal antibody (mAb). Mice were immunized with glucose-6-phosphate isomerase (GPI) and injected intraperitoneally with 2 mg of the anti–IL-6R mAb MR16-1 or control Ig on day 0 (**A**), day 3 (**B**), or day 8 (**C**) or with 4 mg of MR16-1 or control Ig on day 14 (**D**) after GPI immunization. The development of arthritis was monitored visually and scored on a scale of 0–3 (see Materials and Methods for details). Arrow indicates the date of mAb injection. Values are the mean and SEM of 5 mice per group. Results are representative of 2 independent experiments. * = $P < 0.05$ versus controls, by Mann-Whitney U test.

Next, we explored whether anti–IL-17 mAb affects the production of anti-GPI antibodies. Treatment of mice with anti–IL-17 mAb on day 7 or on day 14 did not appreciably affect the titers of anti-GPI antibody (Figure 3B). These results indicate that Th17 cells are involved in the development of GPI-induced arthritis independently of anti-GPI antibody titers.

Inhibition of arthritis by anti–IL-6R mAb. It has been reported that IL-6 plays an important role in the differentiation of Th17 cells from naive T cells (8,9). We speculated that blockade of IL-6 might inhibit the development of arthritis, and we examined the effects of anti–IL-6R mAb MR16-1 on the development of arthritis. We injected 2 mg of MR16-1 intraperitoneally on day 0, 3, or 8 after immunization with recombinant human GPI, or we injected 4 mg on day 14 after immunization. As we anticipated, injection of MR16-1 on day 0 completely blocked the development of arthritis (Figure 4A), and injection on day 3 showed an almost complete inhibition (Figure 4B). Even after the development of arthritis, injection of MR16-1 on day 8 significantly suppressed the progression of arthritis (Figure 4C); however, injection of 4 mg of MR16-1 on day 14, at the peak of arthritis, did not ameliorate arthritis (Figure 4D). These results suggest that blockade of IL-6R has protective effects and some therapeutic effects on GPI-induced arthritis.

Inhibition of the development of Th17 cells, without an increase in Th1, Th2, or Treg cell populations, by anti–IL-6R mAb. To examine whether MR16-1 affects Th1, Th2, and Treg cells, we cultured cells from draining lymph nodes obtained on day 7 in the presence of recombinant human GPI for 24 hours. Since the majority of cells that produce IL-17 are of the $CD4^{high}$ population, we analyzed IFNγ and IL-4 production gating on the $CD4^{high}$ population. We found that the majority of cells that produced cytokines such as IL-17 expressed $CD4^{high}$ cells (data not shown).

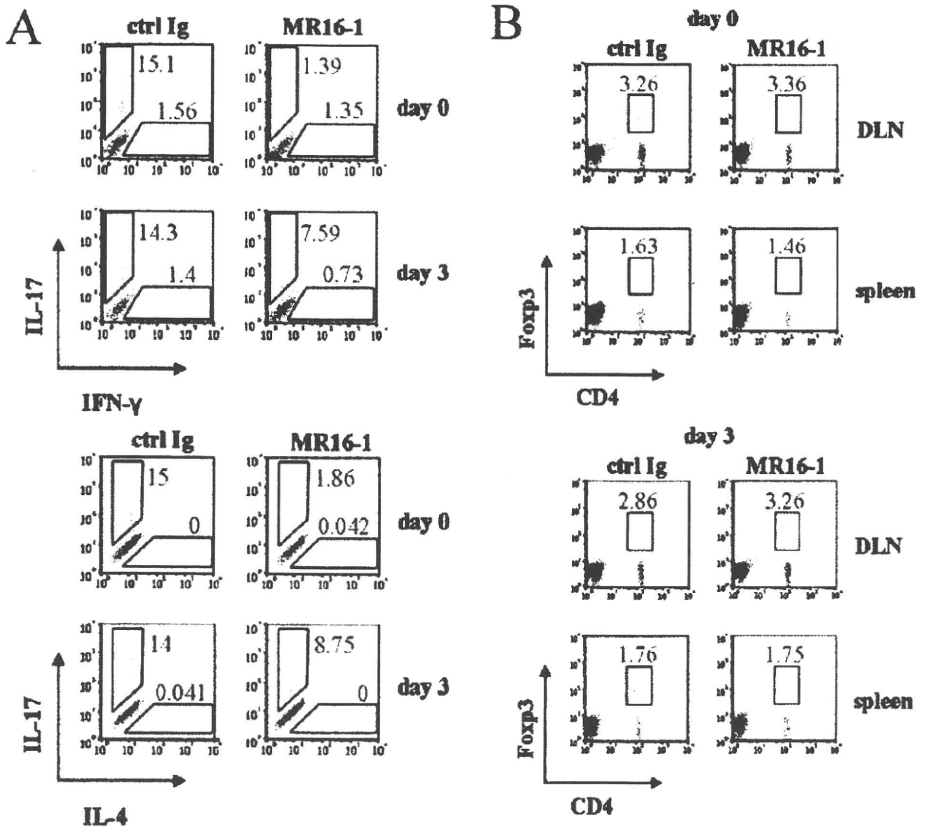

Figure 5. Inhibition of the differentiation of draining lymph node cells into Th17 cells by treatment with anti–interleukin-6 receptor (anti–IL-6R) monoclonal antibody (mAb). Mice were immunized with glucose-6-phosphate isomerase (GPI) and injected intraperitoneally with 2 mg of the anti–IL-6R mAb MR16-1 or with rat IgG (control) on day 0 or day 3 after GPI immunization. **A,** Cells from draining lymph nodes obtained on day 7 were cultured in the presence of 100 μg of recombinant human GPI. GolgiStop was added during the last 2 hours of each culture, and flow cytometric analysis of IL-17 and either interferon-γ (IFNγ) or IL-4 was performed, gating on $CD4^{high}$ cells. Results are representative of 3 independent experiments (n = 2 mice per experiment). **B,** Cells from draining lymph nodes (DLN) and spleen obtained on day 7 were stained with forkhead box P3 (FoxP3), and flow cytometric analysis of FoxP3 and CD4 was performed. Results are representative of 3 independent experiments (n = 2 mice per experiment). Values shown in the dot plots are the percentages of positive cells in the compartment.

We performed intracellular cytokine staining for IL-17, IFNγ, and IL-4 without nonspecific stimulants, such as phorbol myristate acetate or ionomycin, to assess physiologic cytokine production. Injection of MR16-1 on day 0 resulted in a significant decrease in IL-17 production by $CD4^{high}$ T cells (1.39%) as compared with injection of control Ig (15.1%) ($P < 0.05$), and there was a similar tendency with injection on day 3 (7.59% versus 14.3%; $P < 0.05$) (Figure 5A). IFNγ production was not significantly increased by MR16-1 injection on day 0 (1.35% versus 1.56%) or on day 3 (0.73% versus 1.4%) (Figure 5A). There was no difference in IL-4 production (Figure 5A).

We also used intracellular staining methods to examine FoxP3 expression after treatment with MR16-1. FoxP3-positive CD4+ T cells were essentially unaffected by MR16-1 treatment on day 0 or day 3 (Figure 5B). These data indicate that MR16-1 prevents the differentiation of naive T cells to Th17 cells, but does not affect other cell lineages.

Inhibition of the production of antigen-specific antibodies and antigen-specific proliferation of CD4+ T cells by anti–IL-6R mAb. We next explored whether MR16-1 affects the production of anti-GPI antibodies. Treatment of mice with MR16-1 resulted in significant

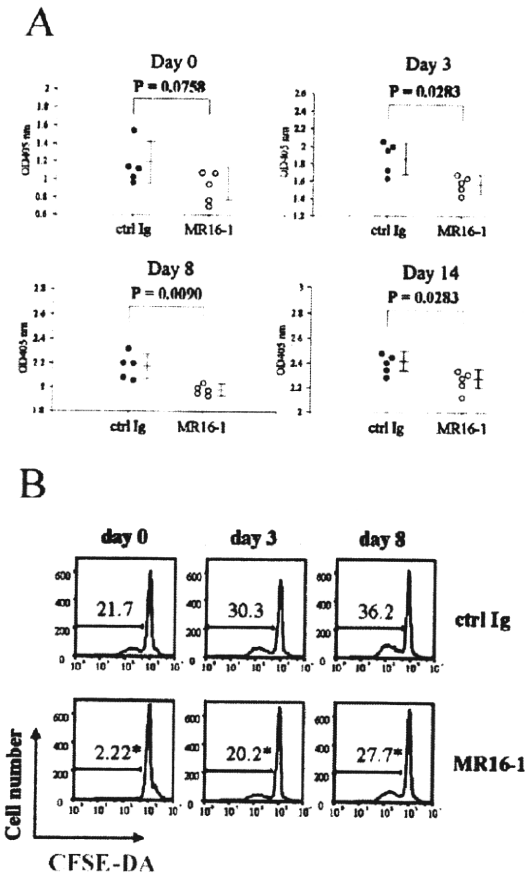

Figure 6. Inhibition of the production of anti–glucose-6-phosphate isomerase (anti-GPI) antibodies and the proliferation of CD4+ T cells by treatment with anti–interleukin-6 receptor (anti–IL-6R) monoclonal antibody (mAb). **A,** Mice were immunized with glucose-6-phosphate isomerase (GPI) and injected intraperitoneally with 2 mg of the anti–IL-6R mAb MR16-1 or rat IgG (control) on day 0, 3, or 8, or with 4 mg of mAb MR16-1 or control Ig on day 14 after GPI immunization. Sera were obtained on day 28, and the titers of anti-GPI antibodies were analyzed by enzyme-linked immunosorbent assay. Each symbol represents a single mouse. Bars show the mean ± SD optical density (OD) at 405 nm. *P* values were determined by Mann-Whitney U test. **B,** Mice were injected intraperitoneally with 2 mg of mAb MR16-1 or rat IgG (control) on day 0, 3, or 8 after immunization. Cells from draining lymph nodes (DLN) obtained on day 10 were stained with carboxyfluorescein diacetate succinimidyl ester (CFSE-DA), cultured with 25 μg of recombinant human GPI for 60 hours, and cell proliferation was analyzed by flow cytometry. Values are the percentage of proliferating cells. Results are representative of 3 independent experiments (n = 2 mice per experiment). * = $P < 0.05$ versus controls, by Mann-Whitney U test.

reductions of anti-GPI antibody titers on days 3, 8, and 14 ($P < 0.0283$, $P < 0.0090$, $P < 0.0283$, respectively) as compared with mice injected with control Ig (Figure 6A). These results emphasize the inhibitory effects of MR16-1 on the production of anti-GPI antibodies irrespective of the phase of arthritis when treatment is administered.

In addition to antibody production, IL-6 is involved in T cell proliferation (10). Therefore, we explored whether MR16-1 affects antigen-specific proliferation of CD4+ T cells. Mice were injected intraperitoneally with 2 mg of MR16-1 on day 0, 3, or 8 after immunization of recombinant human GPI. Popliteal lymph nodes were harvested on day 10, cells stained with CFSE-DA were cultured with recombinant human GPI for 60 hours, and cell proliferation was analyzed by flow cytometry. As expected, CD4+ T cells treated with MR16-1 in vivo proliferated significantly less than those treated with control IgG (21.7% versus 2.22% on day 0, 30.3% versus 20.2% on day 3, 36.2% versus 27.7% on day 8) ($P < 0.05$) (Figure 6B). These data suggest that MR16-1 inhibits antigen-specific proliferation of CD4+ T cells, leading to a reduced population of antigen-specific CD4+ T cells in draining lymph nodes.

DISCUSSION

GPI, a ubiquitous glycolytic enzyme, is a new candidate autoantigen in the initiation of autoimmune arthritis (2). The arthritogenicity of GPI was first described in T cell receptor–transgenic K/BxN mice (2). In K/BxN mice, CD4+ T cells (especially KRN T cells) were required for the development of arthritis, although they appeared to be dispensable after the mice produced arthritogenic autoantibodies to GPI (11). While the K/BxN mouse is a striking model of spontaneous arthritis, the effectiveness of biologic agents used to treat the arthritis is limited. Tumor necrosis factor α (TNFα) blockade had no effect on the development and progression of arthritis in K/BxN mice (12), and serum transfer from arthritic K/BxN mice into IL-6–deficient mice did not affect the course of arthritis as compared with that in wild-type mice (13).

GPI-induced arthritis is produced by immunization of genetically unaltered DBA/1 mice with GPI. In GPI-induced arthritis, administration of either anti-TNFα mAb or CTLA-4Ig after the onset of arthritis shows a significant amelioration of the arthritis (Matsumoto I, et al: unpublished observations). This model is different from the CIA model in a T cell–dependent manner. In GPI-induced arthritis, administration of anti-CD4 mAb around the time of immunization was shown to completely prevent arthritis, and more noteworthy, administration of anti-CD4 mAb on day 11 and

on day 14 was shown to induce rapid remission of the arthritis (3). These findings highlight the importance of CD4+ T cells in the induction phase and the effector phase of GPI-induced arthritis. In contrast, in CIA, CD4+ T cells are indispensable only until the B cells produce autoantibodies, since anti-CD4 mAb treatment is ineffective when administered after anti-GPI antibodies have appeared (4,5). Judging from these findings, GPI-induced arthritis is considered a useful murine model for analyzing the role of CD4+ T cells in the effector phase of the arthritis.

Several studies have examined the roles of Th17 cells, a distinct lineage of CD4+ effector T cells, in various arthritis models (14–17). CIA was shown to be partially suppressed in IL-17–deficient mice (16), whereas it was exacerbated in IFNγ-deficient mice or IFNγ receptor–deficient mice (18–20). Despite the similarity of Th1 and Th17, the efficacy of anti–IL-17 mAb treatment in GPI-induced arthritis was more marked than in CIA. In the CIA model, administration of anti–IL-17 antibodies during the induction phase of arthritis was shown to only partially inhibit the development of arthritis (21). This difference between GPI-induced arthritis and CIA may reflect a more substantial contribution from cells of the Th17 lineage. In our experiments, the production of IL-17 on day 7 was higher than that on day 14, and for IFNγ, the inverse was true, with lower production of IFNγ on day 7 than on day 14. It has been reported that IFNγ suppresses the production of IL-17 by inhibiting IL-23R (22,23); therefore, a cytokine milieu in which little IFNγ is present during the induction phase of arthritis might boost the production of a large amount of IL-17, and conversely, a milieu in which large amounts of IFNγ are present during the effector phase of arthritis might inhibit the production of IL-17. This might also account for the fact that spontaneous remission began on day 14 in mice with GPI-induced arthritis.

Recent in vitro studies indicated that IL-6 is an essential inducer of the differentiation of Th17 cells (8,9). In our experiments, blockade of IL-6R on days 0 and 3 markedly suppressed the production of IL-17 and the proliferation of GPI-specific CD4+ T cells in vivo. In contrast, GPI-induced arthritis was suppressed by MR16-1 administration on days 0 and 3, and when MR16-1 was administered on day 8, the arthritis was ameliorated, which likely occurred through inhibition of T cell proliferation and autoantibody production, rather than blockade of Th17 differentiation. MR16-1 also suppressed autoantibody production most significantly when administered on day 8. This effect was probably mediated through a direct action on B cells (24,25) because the production of anti-GPI antibodies was highest around day 8 (Matsumoto I, et al: unpublished observations).

In the present experiments, the dose of MR16-1 we administered was 20–40 times higher than the dose of the anti–IL-17 mAb. MR16-1 is a mAb against murine IL-6R, and for there to be sufficient inhibition of the biologic activity of IL-6 in vivo, soluble IL-6 receptors, which are consistently present in the blood, would have to be blocked. Therefore, a relatively high dose would be needed compared with the titer of antibodies to the cytokine itself. This idea is supported by our unpublished data (Matsumoto I, et al: unpublished observations) showing that MR16-1 inhibited the biologic activity of IL-6 in vitro when administered at the same concentration as other antibodies to the cytokine itself.

Are these scenarios applicable to RA in humans? The therapeutic effects of a humanized anti–IL-6Rα antibody (tocilizumab) on RA have recently been reported (26,27). Patients with severe forms of RA retained high titers of anti-GPI antibodies (7,28,29), although a few control subjects also had these antibodies. In anti-GPI antibody–positive individuals, GPI-reactive CD4+ T cells, especially Th1-type cells, were specifically detected in peripheral blood mononuclear cells from RA patients who shared either the HLA–DR*0405 or *0901 haplotype (30). What about mice with GPI-induced arthritis? High titers of anti-GPI antibodies have been found to be produced by arthritis-resistant C57BL/6 mice as well, although their T cells exhibited weak GPI responses (ref. 3 and Matsumoto I, et al: unpublished observations) as compared with the responses of T cells from arthritis-susceptible DBA/1 mice.

These findings indicate that anti-GPI antibodies are not sufficient for the induction of arthritis; it is probable that the support of antigen-specific T cell activation is indispensable. In this regard, GPI-induced arthritis seems to be a useful model for analyzing the pathology of RA in humans. In addition, it has been shown that TNF antagonists clearly inhibit the progression of GPI-induced arthritis (3), even after clinical onset of disease (Matsumoto I, et al: unpublished observations). In our present study, administration of anti–IL-17 mAb or MR16-1 on day 14 (late effector phase) was not able to ameliorate GPI-induced arthritis. However, both the IL-6/IL-17 axis and TNFα might play a crucial role in established RA, since both tocilizumab and TNF antagonists have shown marked therapeutic efficacy in humans with established RA (26,27,31–34), although administration of MR16-1 or anti-TNF mAb has shown no effect or only a weak effect on fully established CIA in mouse models (35,36). Further ana-

lysis is necessary to determine whether GPI-reactive Th17 cells exist in the peripheral blood or joints of patients with RA who have anti-GPI antibodies.

In conclusion, the findings of our study highlight the importance of the IL-6/IL-17 axis in GPI-induced arthritis, a murine model of RA. Blockade of IL-6R might be a useful therapeutic strategy in Th17-mediated arthritis. Since a humanized anti–IL-6R mAb has been shown to have an excellent therapeutic effect on RA, further studies are needed to confirm that the IL-6/IL-17 axis is also crucial in RA.

AUTHOR CONTRIBUTIONS

Dr. Matsumoto had full access to all of the data in the study and takes responsibility for the integrity of the data and the accuracy of the data analysis.

Study design. Iwanami, Matsumoto, Sumida.
Acquisition of data. Iwanami, Matsumoto, Tanaka-Watanabe, Inoue, Mihara, Ohsugi, Mamura, Goto, Ito, Tsutsumi, Kishimoto, Sumida.
Analysis and interpretation of data. Iwanami, Matsumoto, Sumida.
Manuscript preparation. Iwanami, Matsumoto, Sumida.
Statistical analysis. Iwanami, Matsumoto.

REFERENCES

1. Kouskoff V, Korganow AS, Duchatelle V, Degott C, Benoist C, Mathis D. Organ-specific disease provoked by systemic autoreactivity. Cell 1996;87:811–22.
2. Matsumoto I, Staub A, Benoist C, Mathis D. Arthritis provoked by linked T and B recognition of a glycolytic enzyme. Science 1999;286:1732–5.
3. Schubert D, Maier B, Morawietz L, Krenn V, Kamradt T. Immunization with glucose-6-phosphate isomerase induces T cell-dependent peripheral polyarthritis in generally unaltered mice. J Immunol 2004;172:4503–9.
4. Ranges GE, Sriram S, Cooper SM. Prevention of type II collagen-induced arthritis by in vivo treatment with anti-L3T4. J Exp Med 1985;162:1105–10.
5. Williams RO, Whyte A. Anti-CD4 monoclonal antibodies suppress murine collagen-induced arthritis only at the time of primary immunization. Cell Immunol 1996;170:291–5.
6. Tada Y, Ho A, Koh DR, Mak TW. Collagen-induced arthritis in CD4- or CD8-deficient mice: CD8 T cells play a role in initiation and regulate recovery phase of collagen-induced arthritis. J Immunol 1996;156:4520–6.
7. Matsumoto I, Lee DM, Goldbach-Mansky R, Sumida T, Hitchon CA, Schur PH, et al. Low prevalence of antibodies to glucose-6-phosphate isomerase in patients with rheumatoid arthritis and a spectrum of other chronic autoimmune disorders. Arthritis Rheum 2003;48:944–54.
8. Bettelli E, Carrier Y, Gao W, Korn T, Strom TB, Oukka M, et al. Reciprocal developments pathways for the generation of pathogenic effector T_H17 and regulatory T cells. Nature 2006;441:235–8.
9. Mangan PR, Harrington LE, O'Quinn DB, Helms WS, Bullard DC, Elson CO, et al. Transforming growth factor-β induces development of the T_H17 lineage. Nature 2006;441:231–4.
10. Takeda K, Kaisho T, Yoshida N, Takeda J, Kishimoto T, Akira S. Stat 3 activation is responsible for IL-6 dependent T cell proliferation through preventing apoptosis: generation and characterization of T cell-specific Stat3-deficient mice. J Immunol 1998;161:4652–60.
11. Korganow AS, Ji H, Mangialaio S, Duchatelle V, Pelanda R, Martin T, et al. From systemic T cell self-reactivity to organ-specific autoimmune disease via immunoglobulins. Immunity 1999;10:451–61.
12. Kyburz D, Carson DA, Corr M. The role of CD40 ligand and tumor necrosis factor α signaling in the transgenic K/BxN mouse model of rheumatoid arthritis. Arthritis Rheum 2000;43:2571–7.
13. Ji H, Pettit A, Ohmura K, Ortiz-Lopez A, Duchatelle V, Degott C, et al. Critical roles for interleukin 1 and tumor necrosis factor α in antibody-induced arthritis. J Exp Med 2002;196:77–85.
14. Nakae S, Nambu A, Sudo K, Iwakura Y. Suppression of immune induction of collagen-induced arthritis in IL-17-deficient mice. J Immunol 2003;171:6173–7.
15. Nakae S, Saijo S, Horai R, Sudo K, Mori S, Iwakura Y. IL-17 production from activated T cells is required for the spontaneous development of destructive arthritis in mice deficient in IL-1 receptor antagonist. Proc Natl Acad Sci U S A 2003;100:5986–90.
16. Koenders MI, Lubberts E, Oppers-Walgreen B, van den Bersselaar L, Helsen MM, Di Padova FE, et al. Blocking of interleukin-17 during reactivation of experimental arthritis prevents joint inflammation and bone erosion by decreasing RANKL and interleukin-1. Am J Pathol 2005;167:141–9.
17. Koenders MI, Kolls JK, Oppers-Walgreen B, van den Bersselaar L, Joosten LA, Schurr JR, et al. Interleukin-17 receptor deficiency results in impaired synovial expression of interleukin-1 and matrix metalloproteinase 3, 9, and 13 and prevents cartilage destruction during chronic reactivated streptococcal cell wall–induced arthritis. Arthritis Rheum 2005;52:3239–47.
18. Chu CQ, Song Z, Mayton L, Wu B, Wooley PH. IFNγ deficient C57BL/6 (H-2^b) mice develop collagen induced arthritis with predominant usage of T cell receptor Vβ6 and Vβ8 in arthritic joints. Ann Rheum Dis 2003;62:983–90.
19. Manoury-Schwartz B, Chiocchia G, Bessis N, Abehsira-Amar O, Batteux F, Muller S, et al. High susceptibility to collagen-induced arthritis in mice lacking IFN-γ receptors. J Immunol 1997;158:5501–6.
20. Vermeire K, Heremans H, Vandeputte M, Huang S, Billiau A, Matthys P. Accelerated collagen-induced arthritis in IFN-γ receptor-deficient mice. J Immunol 1997;158:5507–13.
21. Lubberts E, Koenders MI, Oppers-Walgreen B, van den Bersselaar L, Coenen-de Roo CJ, Joosten LA, et al. Treatment with a neutralizing anti-murine interleukin-17 antibody after the onset of collagen-induced arthritis reduces joint inflammation, cartilage destruction, and bone erosion. Arthritis Rheum 2004;50:650–9.
22. Harrington JE, Hatton RD, Mangan PR, Turner H, Murphy TL, Murphy KM, et al. Interleukin-17-producing $CD4^+$ effector T cells develop via a lineage distinct from the T helper type 1 and 2 lineages. Nat Immunol 2005;6:1123–32.
23. Park H, Li Z, Yang XO, Chang SH, Nurieva R, Wang Y, et al. A distinct lineage of CD4 T cells regulates tissue inflammation by producing interleukin 17. Nat Immunol 2005;6:1133–41.
24. Muraguchi A, Kishimoto T, Miki Y, Kuritani T, Kaieda T, Yoshizaki K, et al. T cell-replacing factor (TRF)-induced IgG secretion in human B blastoid cell line and demonstration of acceptors for TRF. J Immunol 1981;127:412–6.
25. Yoshizaki K, Nakagawa T, Kaieda T, Muraguchi A, Yamamura Y, Kishimoto T. Induction of proliferation and Igs-production in human B leukemic cells by anti-immunoglobulins and T cell factors. J Immunol 1982;128:1296–301.
26. Choy EH, Isenberg DA, Garrood T, Farrow S, Ioannou Y, Bird H, et al. Therapeutic benefit of blocking interleukin-6 activity with an anti–interleukin-6 receptor monoclonal antibody in rheumatoid arthritis: a randomized, double-blind, placebo-controlled, dose-escalation trial. Arthritis Rheum 2002;46:3143–50.
27. Nishimoto N, Yoshizaki K, Miyasaka N, Yamamoto K, Kawai S, Takeuchi T, et al. Treatment of rheumatoid arthritis with human-

ized anti–interleukin-6 receptor antibody: a multicenter, double-blind, placebo-controlled trial. Arthritis Rheum 2004;50:1761–9.
28. Schaller M, Burton DR, Ditzel HJ. Autoantibodies to GPI and creatine kinase in RA, and few human autoimmune sera detect GPI. Nat Immunol 2002;3:412–3.
29. Van Gaalen FA, Toes RE, Ditzel HJ, Schaller M, Breedveld FC, Verweij CL, et al. Association of autoantibodies to glucose-6-phosphate isomerase with extraarticular complications in rheumatoid arthritis. Arthritis Rheum 2004;50:395–9.
30. Kori Y, Matsumoto I, Zhang H, Yasukochi T, Hayashi T, Iwanami K, et al. Characterisation of Th1/Th2 type, glucose-6-phosphate isomerase reactive T cells in the generation of rheumatoid arthritis. Ann Rheum Dis 2006;65:968–9.
31. Maini R, St.Clair EW, Breedveld F, Furst D, Kalden J, Weisman M, et al, for the ATTRACT Study Group. Infliximab (chimeric anti-tumour necrosis factor α monoclonal antibody) versus placebo in rheumatoid arthritis patients receiving concomitant methotrexate: a randomized phase III trial. Lancet 1999;354:1932–9.
32. Lipsky PE, van der Heijde DM, St.Clair EW, Furst DE, Breedveld FC, Kalden JR, et al, for the Anti–Tumor Necrosis Factor Trial in Rheumatoid Arthritis with Concomitant Therapy Study Group. Infliximab and methotrexate in the treatment of rheumatoid arthritis. N Engl J Med 2000;343:1594–602.
33. Moreland LW, Baumgartner SW, Schiff MH, Tindall EA, Fleischmann RM, Weaver AL, et al. Treatment of rheumatoid arthritis with a recombinant human necrosis factor receptor (p75)-Fc fusion protein. N Engl J Med 1997;337:141–7.
34. Weinblatt ME, Kremer JM, Bankhurst AD, Bulpitt KJ, Fleischmann RM, Fox RI, et al. A trial of etanercept, a recombination tumor necrosis factor receptor:Fc fusion protein, in patients with rheumatoid arthritis receiving methotrexate. N Engl J Med 1999; 340:253–9.
35. Takagi N, Mihara M, Moriya Y, Nishimoto N, Yoshizaki K, Kishimoto T, et al. Blockage of interleukin-6 receptor ameliorates joint disease in murine collagen-induced arthritis. Arthritis Rheum 1998;41:2117–21.
36. Joosten LA, Helsen MM, van de Loo FA, van den Berg WB. Anticytokine treatment of established type II collagen–induced arthritis in DBA/1 mice: a comparative study using anti-TNFα, anti-IL-1α/β, and IL-1Ra. Arthritis Rheum 1996;39:797–809.

Lack of lacto/neolacto-glycolipids enhances the formation of glycolipid-enriched microdomains, facilitating B cell activation

Akira Togayachi[a], Yuko Kozono[a], Yuzuru Ikehara[a], Hiromi Ito[a], Nami Suzuki[a], Yuki Tsunoda[a], Sumie Abe[a], Takashi Sato[a], Kyoko Nakamura[b], Minoru Suzuki[b], Hatsumi M. Goda[c], Makoto Ito[c], Takashi Kudo[d], Satoru Takahashi[d], and Hisashi Narimatsu[a,1]

[a]Research Center for Medical Glycoscience, National Institute of Advanced Industrial Science and Technology, Central-2 OSL, 1-1-1 Umezono, Tsukuba, Ibaraki 305-8568, Japan; [b]Sphingolipid Expression Laboratory, Supra-Biomolecular System Research Group, RIKEN Frontier Research System, 2-1 Hirosawa, Wako, Saitama 351-0198, Japan; [c]Department of Bioscience and Biotechnology, Graduate School of Bioresource and Bioenvironmental Sciences, Kyushu University, 6-10-1 Hakozaki, Higashi-ku, Fukuoka 812-8581, Japan; and [d]Department of Anatomy and Embryology, Graduate School of Comprehensive Human Sciences, University of Tsukuba, 1-1-1 Tennodai, Tsukuba, Ibaraki 305-8575, Japan

Edited* by Senitiroh Hakomori, Pacific Northwest Research Institute, Seattle, WA, and approved May 10, 2010 (received for review December 16, 2009)

In a previous study, we demonstrated that β1,3-*N*-acetylglucosaminyltransferase 5 (*B3gnt5*) is a lactotriaosylceramide (Lc_3Cer) synthase that synthesizes a precursor structure for lacto/neolacto-series glycosphingolipids (GSLs) in in vitro experiments. Here, we generated *B3gnt5*-deficient (*B3gnt5*$^{-/-}$) mice to investigate the in vivo biological functions of lacto/neolacto-series GSLs. In biochemical analyses, lacto/neolacto-series GSLs were confirmed to be absent and no Lc_3Cer synthase activity was detected in the tissues of these mice. These results demonstrate that β3GnT5 is the sole enzyme synthesizing Lc_3Cer in vivo. Ganglioside GM1, known as a glycosphingolipid-enriched microdomain (GEM) marker, was found to be upregulated in *B3gnt5*$^{-/-}$ B cells by flow cytometry and fluorescence microscopy. However, no difference in the amount of GM1 was observed by TLC-immunoblotting analysis. The GEM-stained puncta on the surface of *B3gnt5*$^{-/-}$ resting B cells were brighter and larger than those of WT cells. These results suggest that structural alteration of GEM occurs in *B3gnt5*$^{-/-}$ B cells. We next examined whether BCR signaling-related proteins, such as BCR, CD19, and the signaling molecule Lyn, had moved into or out of the GEM fraction. In *B3gnt5*$^{-/-}$ B cells, these molecules were enriched in the GEM fraction or adjacent fraction. Moreover, *B3gnt5*$^{-/-}$ B cells were more sensitive to the induction of intracellular phosphorylation signals on BCR stimulation and proliferated more vigorously than WT B cells. Together, these results suggest that lacto/neolacto-series GSLs play an important role in clustering of GEMs and tether-specific proteins, such as BCR, CD19, and related signaling molecules to the GEMs.

β1,3-*N*-acetylglucosaminyltransferase | glycosyltransferase | polylactosamine | glycosphingolipid | B cell receptor

Almost all organisms possess lipids and proteins to which a broad range of carbohydrate chains are linked. Some carbohydrate structures are known to participate in vital processes, such as the molecules responsible for cell–cell, receptor–ligand, and carbohydrate–carbohydrate interactions. It is known that glycosphingolipids (GSLs) have an important role in biological functions. In mammals, GSLs can be classified into several major classes, such as globo-, isoglobo-, ganglio-, and lacto/neolacto-series GSLs and others (Fig. S1). Gangliosides that contain one or more sialic acids on their carbohydrate chains modulate the responsiveness of signaling molecules and cell surface receptors (1). Some functional carbohydrate antigens, such as blood group Lewis antigens and the HNK-1 antigen, are carried on lacto/neolacto-series GSLs. During the development of hematopoietic cells, expression of HNK-1 (CD57) and Lewis-related antigens on lacto/neolacto-series GSLs is spatially and temporally regulated; the expression of such GSLs is also dramatically changed during the immune response (2).

Membrane microdomains are cholesterol- and GSL-rich components of the plasma membrane, also known as glycosphingolipid-enriched microdomains (GEMs), glycosphingolipid-signaling domains, lipid rafts, detergent-resistant membrane structures (DRMs), or detergent-insoluble glycolipid-enriched complex (3–5). General/classic lipid rafts, referred to here as GEMs, serve as platforms for different mechanisms of cell signaling. GEMs contain other sphingolipids, cholesterol, GPI-anchored proteins, many receptor molecules, and selected signaling molecules. GSLs are major components of GEMs. GSLs in microdomains are involved in various biological functions, such as signal transduction, toxin and infection receptors for bacteria and viruses (6), cell adhesion (5, 7), and cell growth modulation (8). It is thought that the most probable function exerted by GSLs in microdomains is to concentrate proteins that play a role in transmembrane signaling events and their regulated activation (9). GEMs also contain many important molecules, including immunoreceptors, such as the B cell receptor (BCR), T cell receptor (TCR), CD4, and CD8 among others, as well as cellular signaling molecules (10–14). It is known that GPI-anchored glycoproteins, such as CD48, CD59, and others, are also localized within GEMs. Recent studies have also shown the importance of GEM formation in cell differentiation and the acquired immune response among other processes. In T cells, clustering of GEMs regulates sustained TCR signaling because this process maintains engagement of the TCR with costimulators, such as CD28 and GPI-anchored glycoproteins, leading to partitioning within GEMs and resulting in exclusion of large highly glycosylated proteins, such as CD43 and CD45 (15). For facilitating sustained TCR signal transduction, TCR localization within GEMs results in high local concentrations of TCR signal-related molecules, such as protein tyrosine kinases and signal transducers, and the exclusion of CD45 phosphatase activity, which negatively regulates TCR signaling.

β1,3-*N*-acetylglucosaminyltransferases (β3GnTs) transfer an *N*-acetylglucosamine (GlcNAc) from UDP-GlcNAc to Gal on the nonreducing end of the carbohydrate chain with a β1,3-linkage. At present, eight members of the human β3GnT family have been cloned and characterized (16). In a previous study (17), β3GnT5 was cloned as lactotriaosylceramide (Lc_3Cer) synthase and characterized as a key enzyme for the biosynthesis of lacto/neolacto-series GSLs (17, 18). *B3gnt2* (*β3GnT2*) mRNA is ubiquitously

Author contributions: A.T., Y.K., Y.I., H.I., T.S., T.K., S.T., and H.N. designed research; A.T., Y.K., Y.I., H.I., N.S., Y.T., S.A., K.N., M.S., H.M.G., M.I., T.K., and S.T. performed research; K.N., M.S., H.M.G., and M.I. contributed new reagents/analytic tools; A.T., Y.K., Y.I., H.I., N.S., Y.T., S.A., T.S., K.N., M.S., H.M.G., M.I., T.K., S.T., and H.N. analyzed data; and A.T. and H.N. wrote the paper.

The authors declare no conflict of interest.

*This Direct Submission article had a prearranged editor.

Data deposition: The sequence reported in this paper has been deposited in the GenBank database (accession no. AB045278).

[1]To whom correspondence should be addressed. E-mail: h.narimatsu@aist.go.jp.

This article contains supporting information online at www.pnas.org/lookup/suppl/doi:10.1073/pnas.0914298107/-/DCSupplemental.

expressed in mouse tissues, and thus also in B cells, T cells, and other immune cells. The previous study demonstrated that *B3gnt2*$^{-/-}$ B and T cells, which lack polylactosamine (PLN) on the *N*-glycans of their glycoproteins, showed hyperactivation following BCR or TCR/CD28 stimulation (19). Thus, PLN chains on glycoproteins have an important role in determining thresholds for in vitro immunocyte activation. On the other hand, we and other groups have observed that the expression of *B3gnt5* mRNA is limited mainly to B cells (Fig. S1). We are also interested in the functions of PLN chains not only on glycoproteins but on GSLs in B cells.

It has been reported that disruption of the *B3gnt5* gene leads to preimplantation lethality; therefore, no individuals homozygous for *B3gnt5*-null alleles are viable (20). However, we have succeeded in generating *B3gnt5*-deficient mice by a different approach, for example, by using a different ES cell clone and genomic construction (targeting vector). The *B3gnt5*$^{-/-}$ mice generated in this study were viable and fertile and showed normal growth, although they were *B3gnt5*-null in all tissues tested. Thus, this study on gene-disrupted mice lacks lacto/neolacto-series GSLs. We found that abnormal formation of GEMs was significantly increased in *B3gnt5*$^{-/-}$ mice. This observation prompted us to investigate whether the mice show immunological disorders of B cells and how lacto/neolacto-series GSLs are involved in BCR/CD19 signaling.

Results

Generation of *B3gnt5*$^{-/-}$ Mice. Quantitative real-time RT-PCR analysis confirmed that *B3gnt5* mRNA expression was present at a high level in immune organs and/or cells (Fig. S1). To analyze whether disorders of the immune system would occur in its absence, we generated *B3gnt5*-deficient mice.

To confirm the generation of *B3gnt5*-deficient mice, we analyzed expression of the *B3gnt5* gene and lactotriaosylceramide (Lc_3Cer)-synthesizing activity in the tissues of WT and *B3gnt5*$^{-/-}$ mice. Previously, we reported that the HL-60 cell line expressed abundant *B3gnt5* transcripts, whereas the Jurkat cell line did not (17). In Fig. 1, tissue homogenates of WT mice showed apparent activity of Lc_3Cer synthase in all organs except the cerebrum. This is consistent with a previous report by others in which the adult cerebral cortex was found to express little or no *B3gnt5* transcript. In contrast, the adult cerebellum expresses *B3gnt5* transcripts at a comparatively high level in Purkinje cells (18). Tissue homogenates of *B3gnt5*$^{-/-}$ mice exhibited no Lc_3Cer-synthesizing activity. These results indicate that there is no other glycosyltransferase with Lc_3Cer-synthesizing activity.

Glycan Structure of GSLs Extracted from Tissues of WT and *B3gnt5*-Deficient Mice. We performed TLC-immunoblotting using anti-GlcNAc Ab (kindly provided by Minoru Suzuki, RIKEN, Saitama, Japan) on GSLs from the cerebellum. Orcinol staining revealed no differences in the patterns of GSLs (Fig. S2). This is probably attributable to the low content of lacto/neolacto-series GSLs as compared with gangliosides. However, the immunoblotting results shown in Fig. S2 clearly demonstrated that Lc_3Cer (amino-CTH) was absent in the *B3gnt5*$^{-/-}$ cerebellum. On the other hand, we could not detect the signal for Lc_3Cer on TLC (-immunoblotting) analysis of spleen, probably because the amount of Lc_3Cer was too low in total GSLs. Orcinol staining again showed no difference between WT and *B3gnt5*$^{-/-}$ mice in acidic GSLs from spleen (Fig. S2). By immunostaining the acid fraction of GSLs treated with sialidase, at least three positive bands were detected in WT spleen using the 1B2-1B7 mAb (Fig. S2). These bands entirely disappeared in *B3gnt5*$^{-/-}$ mice. It is known that mAb 1B2-1B7 reacts with neolactotetraosylceramide (nLc_4Cer), nLc_6Cer, and other glycolipids having LacNAc units at the nonreducing end of their carbohydrate chains.

As seen from the results of MS analysis (Fig. 1 and Fig. S2), we confirmed the loss of elongated GSLs on Lc_3Cer in *B3gnt5*$^{-/-}$ B cells. Signals of nos. 7 and 16 were absent in *B3gnt5*$^{-/-}$ mice, although they were present in WT B cells. No. 7 was identified as

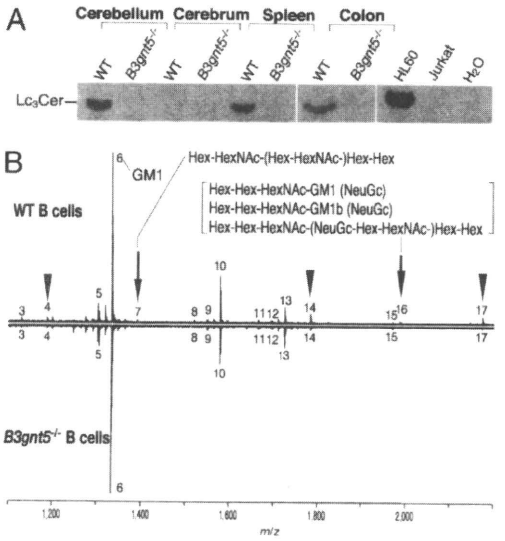

Fig. 1. Confirmation of Lc_3Cer synthase activity in *B3gnt5*$^{-/-}$ mice and MS analysis of the glycans derived from GSLs of mouse B cells. (*A*) Homogenates (100 μg of protein) of mouse tissues were used to assay Lc_3Cer synthase activity. The products were separated on a high-performance twin-layer chromatography (HPTLC) plate with a solvent system of chloroform/methanol/0.2% $CaCl_2$ (60:35:8 vol/vol/vol). The intensities of the radioactive bands were measured with a FLA3000 Image Analyzer (Fujifilm, Tokyo). HL-60, which has Lc_3Cer synthase activity, and Jurkat, which does not, were used as positive and negative controls, respectively. Lc_3Cer synthase assays were performed on two TLC plates, with positive and negative control on each plate. This figure was prepared from the results of two TLC plates to demonstrate Lc_3Cer synthase activity in cerebellum, spleen, and colon between WT and *B3gnt5*$^{-/-}$ mice. (*B*) MS spectra of the glycans derived from GSLs of mouse B cells. Arrows indicate glycan signals that are absent from GSLs of *B3gnt5*$^{-/-}$ B cells. Arrowheads indicate glycan signals that are decreased in GSLs of *B3gnt5*$^{-/-}$ B cells. Table S1 summarizes the results of the assigned GSL-derived glycan structures of mouse B cells. Detailed methods for MS of glycans derived from GSLs are described in Fig. S2.

Galβ1-4GlcNAcβ1-3(Galβ1-4GlcNAcβ1-6)Galβ1-4Glc, which is one of the lacto/neolacto-series GSL structures, using the method described in *SI Experimental Procedures and Results*. The *m/z* (1,987.147) of no. 16 indicates three candidates that are possibly ganglio-series glycolipids or lacto/neolacto-series GSLs, as listed in Table S1. In in vitro recombinant β3GnT5, enzyme acts on ganglio-series GSLs, including GA1, GM1 (GM1a), and GD1b, as an acceptor substrate (18). Therefore, this is likely to be one of the lacto/neolacto-series GSLs having a Hex-Hex-*N*-acetylhexosamine (HexNAc)-[sialic acid (NeuGc)-Hex-HexNAc] Hex-Hex structure and/or one of the ganglio-series GSLs having a Hex-Hex-HexNAc-GM1a structure, because it was absent in the B cells of *B3gnt5*$^{-/-}$ mice. The signals of nos. 4, 14, and 17 (Fig. 1*B* and Fig. S2) significantly decreased in *B3gnt5*$^{-/-}$ B cells. These molecular masses correspond to both ganglio-series and lacto/neolacto-series GSLs, as listed in Table S1. A mixture of both ganglio-series and lacto/neolacto-series GSLs may be contained in these samples, and the lack of lacto/neolacto-series and/or minor ganglio-series GSLs in *B3gnt5*$^{-/-}$ B cells may reflect this.

Flow Cytometry and Immunoblot Analyses of PLN Using *Lycopersicon esculentum* Lectin. Our previous study indicated that of the four members of the β3GnTs, β3GnT2 exhibits the strongest PLN synthetic ability in vitro and that β3GnT5 shows lower activity, ~30% of that of β3GnT2 (17). To examine whether PLN on glycoproteins is affected in *B3gnt5*$^{-/-}$ mice, flow cytometry (FCM) analysis of splenocytes was performed using *Lycopersicon esculentum* (LEL) lectin. This lectin binds to PLN chains having at least three LacNAc repeats. By FCM, no difference between

WT and *B3gnt5*$^{-/-}$ splenocytes and B cells in LEL staining at the cell surface was observed (Fig. S3). As seen in Fig. S3, blotting analysis using LEL showed strong signals for both WT and *B3gnt5*$^{-/-}$ splenocytes without any significant difference of intensity as compared with *B3gnt2*$^{-/-}$ splenocytes. This suggests that β3GnT5 is not involved in the expression of PLN chains on glycoproteins.

FCM Analysis of Hematocytes in *B3gnt5*-Deficient Mice. To investigate whether hematocytes manifest aberrant cell distribution or development in *B3gnt5*$^{-/-}$ mice, we analyzed the expression of a series of CD antigens on the cell surface of peripheral blood and splenic cells using FCM. The antigens investigated were the same as those described in a previous study (19). No significant disturbance in the ratios of cell populations, such as T cells, B cells, monocytes, or granulocytes, was observed. However, we documented a marginal increase in Ab levels in intact mouse serum; the levels of total IgG, IgG_{2a}, and IgG_{2b} were increased in *B3gnt5*$^{-/-}$ mice as compared with WT mice (Fig. S4). Lacto/neolacto-GSLs are known to be localized in GEMs on the cell surface. However, some antibodies that bind to lacto/neolacto-GSLs, such as the anti-LacNAc mAb 1B2-1B7, are known to cross-react with carbohydrate antigens on glycoproteins. Therefore, we investigated GSL antigens on the cell surface (i.e., GM1, GM3, Gb3, others) as GEM markers. In a series of FCM analysis, we were interested to observe that the intensity of GM1 staining with Ab or cholera toxin B subunit (CT-B) was significantly increased in the B cells of *B3gnt5*$^{-/-}$ mice as compared with WT mice (Fig. 2). GM1 levels were increased on splenic B cells (Fig. 2, gate: $CD19^+$ cells) of *B3gnt5*$^{-/-}$ mice [mean fluorescence intensity (MFI) of ~1,431] as compared with WT mice (MFI of ~625).

BCR and CD19 antigens on the B cell surface were not different in WT and *B3gnt5*$^{-/-}$ mice. There was also no difference in the level of expression of these molecules in WT or *B3gnt5*$^{-/-}$ mice, as assessed by Western blotting (Fig. S5). Because it is known that many GPI-anchored proteins are localized in GEMs, we examined the expression profiles of other GPI-anchored proteins, such as CD48. However, we found no differences between WT and *B3gnt5*$^{-/-}$ mice in any expression profiles. In contrast to these findings with B cells, T cells did not manifest any differences in GM1 expression detected by CT-B. This may be interpreted in relation to their initially low expression of *B3gnt5* transcripts.

Microscopic Analysis of GEMs in B Cells. We observed GEM formation on the cell surface using cholera toxin as a probe, because it is known that CT-B binds to GM1. CT-B and various GPI-anchored proteins have been defined and identified previously as components of GEMs. CT-B staining of the cell surface showed a punctate pattern by fluorescence microscopy (Fig. 3). This pattern was identical to that reported in previous studies. In the present study, the puncta on the surface of *B3gnt5*$^{-/-}$ resting B cells were much brighter and larger and their number was significantly increased as compared with WT. These CT-B staining levels for the puncta of *B3gnt5*$^{-/-}$ resting cells were almost as high as for stimulated WT B cells (Fig. 3). Thus, the B cells of *B3gnt5*$^{-/-}$ mice may be easier to activate; furthermore, the staining levels of puncta were increased even more in stimulated B cells of *B3gnt5*$^{-/-}$ mice as compared with stimulated WT cells.

Because GM1 staining on FCM was up-regulated, we examined six transcripts for glycosyltransferase genes involved in the synthesis of GM1 in resting B cells from WT and *B3gnt5*$^{-/-}$ mice. By the comparative PCR method using real-time PCR (Fig. S6), there were no significant differences between the B cells of WT and *B3gnt5*$^{-/-}$ mice in the levels of these six transcripts. No expression of *B3gnt5* mRNA in resting B cells of *B3gnt5*$^{-/-}$ mice could be confirmed. In addition, the pattern of MS spectra indicated no marked change in the amount of GM1, with the exception of the decreased peak intensity related to lacto/neolacto-series GSLs. (Fig. 1 and Fig. S2). However, MS analysis and orcinol staining of GSLs on TLC (Fig. S6) are, in general, poorly

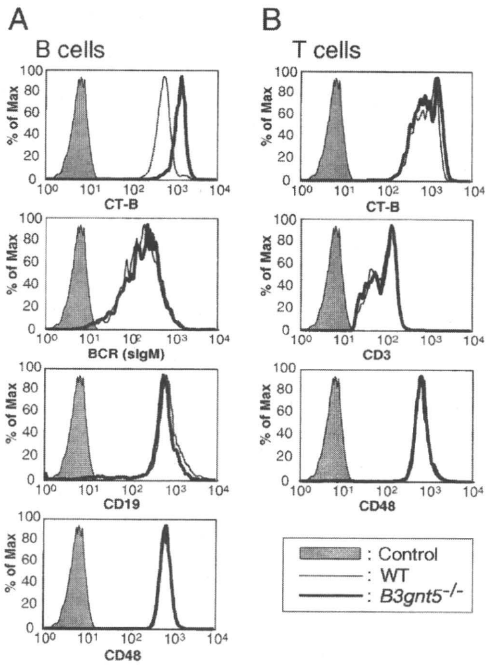

Fig. 2. Up-regulation of CT-B staining as a GEM marker but no alteration of surface protein expression on B cells. FCM analysis of GEMs and surface proteins on splenic B cells (*A*) and T cells (*B*). The expression on the splenocyte cell surface was analyzed by FCM using FITC-conjugated CT-B, anti-CD3ε, anti-BCR (sIgM), anti-CD48 Abs, and phycoerythrin (PE)-conjugated anti-CD19. Results are shown as histograms of fluorescence intensity. The shaded peak in each panel represents the negative control. Max, maximum.

quantitative. Therefore, the total amount of GM1 in B cells was determined by TLC-immunoblotting using HRP-conjugated CT-B. Total amounts of GM1 did not differ between WT and *B3gnt5*$^{-/-}$ mice (Fig. S6).

Distribution Analysis of GEM Proteins. As reported in the previous studies, we observed in this study that BCR, CD19, and Lyn of B cells were colocalized in low-density membrane fraction GEMs (Fig. 4, designated fractions 1–4) prepared in medium containing 1% Triton X-100 and separated by sucrose density gradient centrifugation. We analyzed the behavior of BCR transduction-related proteins in GEMs after stimulation with anti-BCR Ab and anti-CD19 Ab cross-linking (Fig. 4). Western blotting showed that the BCR and CD19 antigens from B cells of *B3gnt5*$^{-/-}$ mice were markedly increased in the GEM fraction, as compared with WT mice. In addition, larger amounts of Lyn kinases were located in the GEM fraction in *B3gnt5*$^{-/-}$ B cells. On the other hand, we determined that not only cross-linking of BCR together with CD19 but cross-linking of CD19 alone resulted in abnormalities in the GEM structure. This suggests that GEM-related molecules, such as BCR, CD19, and Lyn, show increased motility into GEM (fractions 1–4; Fig. S7). These results indicated that *B3gnt5*$^{-/-}$ B cells might be in a state in which they could be more easily activated by external stimuli as compared with WT B cells. We therefore propose that GEM abnormalities are present in *B3gnt5*$^{-/-}$ B cells.

Phosphorylation Signals Under BCR Stimulation Are Increased in B Cells of *B3gnt5*-Deficient Mice. Many kinases have been reported to play important roles in signal transduction following BCR stimulation. To analyze the alteration of BCR downstream signals after anti-BCR cross-linking, we examined phosphorylation patterns in B cells of WT and *B3gnt5*$^{-/-}$ mice. Western blotting with the Ab 4G10, specific for phosphotyrosine, yielded multiple

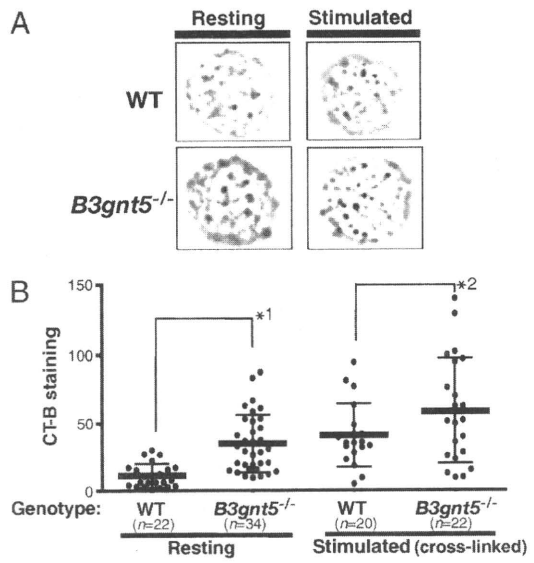

Fig. 3. Fluorescence microscopy of GEMs on the cell surface. (*A*) Fluorescence microscopy showed a CT-B–induced punctate pattern indicating GEM structures on the B cell surface. Resting or stimulated isolated B cells were stained with FITC-conjugated CT-B. The results shown are representative of several independent experiments revealing markedly stronger staining of *B3gnt5*$^{-/-}$ than WT B cells. (*B*) Fluorescence intensity of positive signals for each CT-B–stained punctate region was analyzed by means of a BZ-Analyzer (KEYENCE). The total value of the positive signals on each cell surface was measured. Statistical analysis of the difference between WT and *B3gnt5*$^{-/-}$ B cells, with or without stimulation, was performed using one-way ANOVA and Tukey testing by means of PRISM4 software. Data are given as each cell type's mean (bold line) and SD. *1, $P < 0.01$; *2, $P < 0.01$.

bands (Fig. 5). Immunoblotting with Ab 4G10 showed that tyrosine phosphorylation of multiple proteins in *B3gnt5*$^{-/-}$ B cells was dramatically increased as compared with WT mice.

Enhanced Response of Stimulated *B3gnt5*-Deficient B Cells. BCR and CD19 are major immune receptors and costimulatory molecules, respectively, for B cell activation (21). Because the behavior of these molecules in GEMs was different between WT and *B3gnt5*$^{-/-}$ B cells, we examined the impact of lacto/neolacto-GSL deficiency on B cell proliferation. Resting B cells were stimulated with anti-BCR (anti-IgM) and assessed for proliferation after 2 d. A greater proliferation of *B3gnt5*$^{-/-}$ than WT splenic B cells was observed with low concentrations of anti-BCR (Fig. 5). These results indicate that the lack of PLN in GSLs of B cells lowers the cellular threshold for proliferation triggered by BCR stimulation. In addition, we examined the in vivo response to the T-independent type II antigen [TI-II antigen, trinitrophenol (TNP)-Ficoll]. The specific Ab response to TNP was slightly up-regulated in *B3gnt5*$^{-/-}$ mice (Fig. 5*C*). The levels of IgM production were up-regulated at an early stage of the response in *B3gnt5*$^{-/-}$ mice as compared with WT mice. However, 14 d after immunization, differences between WT and *B3gnt5*$^{-/-}$ mice were no longer apparent in the levels of TNP-specific Ab produced.

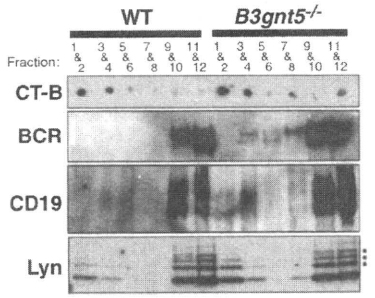

Fig. 4. Distribution of BCR, CD19, and Lyn in GEMs separated into fractions by sucrose density gradient centrifugation. B cells stimulated with anti-BCR and anti-CD19 Abs were lysed with 1% Triton X-100 solubilization buffer. After sucrose gradient centrifugation, fractions were collected from the top of gradient. Then, every second fraction was combined starting from the top fraction. GM1, a GEM marker, was detected using HRP-conjugated CT-B as shown. After fractionation, immunoprecipitation of BCR and CD19 was performed using anti-BCR and anti-CD19 Abs, respectively. BCR (sIgM) and CD19 proteins in *B3gnt5*$^{-/-}$ B cells were up-regulated in the GEM fraction (fractions 1–4). Lyn proteins were also up-regulated in the GEM fraction of *B3gnt5*$^{-/-}$ B cells. The results shown are representative of several independent experiments. *Nonspecific bands.

Discussion

The results of previous studies had strongly indicated that β3GnT5 was the most feasible candidate for the Lc_3Cer synthase (17, 18). We had also determined that mouse B cells expressed abundant *B3gnt5* transcripts and possessed Lc_3Cer synthase activity. To approach the question of the significance of lacto/neolacto-series GSLs in biological function, we generated *B3gnt5*$^{-/-}$ mice. In the present study, we confirmed that Lc_3Cer synthase activity was undetectable in any of the tissue homogenates of *B3gnt5*$^{-/-}$ mice examined. These results indicate that Lc_3Cer synthase is the sole enzyme responsible for the extension of PLN chains on lacto/neolacto-series GSLs.

Lacto/neolacto-series GSLs contain sialic acid or sulfate, resulting in sialylparagloboside, sulfoglucuronylglycolipid, and other

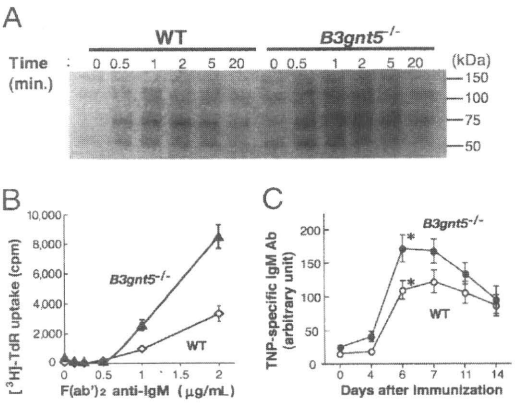

Fig. 5. Analysis of phosphorylation status and enhanced response to BCR cross-linking in resting B cells. (*A*) Resting B cells from spleen were stimulated by cross-linking anti-BCR Ab for the indicated time. The same volume of lysates was added to each lane. Phosphorylated proteins were analyzed by immunoblots using anti-phospho-Tyr mAb (4G10). *B3gnt5*$^{-/-}$ B cells exhibited significantly up-regulated phosphorylation signals. (*B*) Resting B cells from *B3gnt5*$^{-/-}$ mice show enhanced responses to BCR-mediated stimulation. Resting B cells were cultured with the indicated dose of $F(ab')_2$ anti-IgM. Proliferative responses are given as [^{3}H]-thymidine (TdR) incorporation for the final 6 h of the 42-h culture period. Each assay was performed in triplicate, and all data are representative of three experiments. Open circles indicate WT mice, and closed triangles indicate *B3gnt5*$^{-/-}$ mice. (*C*) Response to TI-II antigen. Mice were immunized i.p. with 25 μg of TNP-Ficoll in PBS at day 0. Sera were collected sequentially from the eye socket and tested at a 1:100 dilution. The levels of TNP-specific IgM Ab in sera were determined by ELISA. Representative data were obtained for five (WT) and six (*B3gnt5*$^{-/-}$) mice, respectively. Open circles indicate WT mice, and closed circles indicate *B3gnt5*$^{-/-}$ mice. Statistical analysis of the difference between WT and *B3gnt5*$^{-/-}$ B cells with days after stimulation was performed by two-way ANOVA using PRISM4 software. The levels of IgM in serum are presented as mean (symbols) ± SE. *$P < 0.05$.

similar derivatives. Mouse lymphocytes contain globo-series GSLs (Gb3 and Gb4) and ganglio-series GSL (GM3) (22), but it was not known whether they possessed neolacto-series GSLs. There is a report that human B cells contain nLc_4Cer (paragloboside) (23). In the present study, we demonstrated that three major GSL bands, which were detected by the 1B2-1B7 mAb after sialidase treatment, were absent from the splenocytes of *B3gnt5*$^{-/-}$ mice. This was confirmed by MS showing the absence of branching structures elongated on Lc_3Cer.

We investigated whether lacto/neolacto-series GSLs have an important role in biological functions, particularly in the immune system. The results indicated that *B3gnt5*$^{-/-}$ mice showed an enhanced response to BCR/CD19 stimuli. Recent studies have shown the importance of appropriate GEM formation for cell activation. Incorporation of a number of receptors, including the BCR, TCR, and GM1, into GEMs constitutes an important step in receptor function. After stimulation with various different agents, receptors and signaling molecules are incorporated into GEMs, effectively accumulate, and interact to result in signal transduction from the site of aggregation (i.e., GEMs). In T cells, aggregation of GEMs by cross-linking with CT-B, analogous to TCR cross-linking, induces signaling events and the respective signaling molecules are phosphorylated (24). We observed higher levels of CT-B staining (Fig. 2) and higher levels of GEM aggregation (Fig. 3) in resting *B3gnt5*$^{-/-}$ B cells, which could be the reason for their enhanced response to BCR stimulation. Because there were no differences in the total amount of GM1 and BCR-related molecules (e.g., BCR, CD19, Lyn), we hypothesize that some abnormalities or alterations of GEM microstructure might have occurred. We found that there was no increased expression of genes relating to the biosynthesis of GM1. This finding indicates that GM1 synthesis was not up-regulated at the level of gene expression. In addition, on the basis of the results of MS glycan analysis, as shown in Fig. 1 and Fig. S2, lacto/neolacto-series GSLs are present as a minor component of total GSLs. On the other hand, GM1 is the major component of total GSLs in mouse B cells. In fact, the pattern of MS spectra indicated no marked change in the amount of GM1, except for the decreased peak intensity related to lacto/neolacto-series GSLs. Nonetheless, the data raise the possibility that acceptor substrate (i.e., lactosylceramide) is shifted from the lacto/neolacto-series GSL synthetic pathway to the GM1 synthetic pathway. However, lacto/neolacto-series GSLs are normally only minor components in total GSLs, and it is difficult to accept that they are the reason for the increase in GM1. MS analysis or orcinol staining on TLC is, in general, poorly quantitative. Therefore, we performed TLC-immunoblotting as a more quantitative mode of analysis of GM1 GSL (Fig. S6). The results demonstrated that the total amount of GM1 did not differ between WT and *B3gnt5*$^{-/-}$ mice.

Concerning the brighter CT-B staining, we speculate that the alteration of GEM microstructure may cause the "unmasking" of GM1. Another possibility is that the alteration of GEM microstructure may affect the accessibility of GM1 molecules for CT-B. The clustering effect of GM1, caused by the ease of patching of GEM, may enhance the staining of CT-B. By immunoblotting, we observed slightly increased CT-B staining in separated GEM fractions. We interpret this as the result of the biochemical isolation of GM1 in clustered (patched) GEMs, as shown in Fig. 3. It is known that the microstructure of GEMs reflects their biochemical characteristics and that GM1 in clustered GEMs differs from monomolecular GM1. In general, lectin-like proteins, which can bind to glycans, exhibit stronger affinity to multivalent ligands than to monovalent ligands. CT-B is also known to form pentamer structures (25). It is possible that the clustered GEMs might be easily (and strongly) stained with CT-B in Figs. 2 and 3. However, we have not obtained enough evidence to explain the changes in GEM microstructure at this time. Although GEMs have been studied by a large number of groups, relatively little is known about their biochemical characteristics. Further study is therefore required to identify the detailed biological functions of ganglioside and GEMs.

One important issue in GEM function is their aggregation. There is now a consensus that GEMs are too small to be observed by light microscopy before stimulation (26). It is also reported that GEM formation is reversible, so that they exist only as transiently stabilized structures. GEMs can coalesce on clustering of their components, such as the BCR in B cells, with ligands, antibodies, and/or proteins having lectin activity. The small individual GEMs cluster into larger, visible, and functional units; such clustering facilitates efficient interaction of GEM-associated proteins. In the case of GPI-anchored proteins, such as CD59, dynamic and transient recruitment of GM1 to CD59 clusters was observed by single-molecule tracking and taken to suggest the involvement of GEMs in signal transduction (27). In this case, to form GEMs, clustering of such receptor molecules causes gathering of cholesterol and GSLs, such as GM1, around themselves. On the other hand, cross-linking of GM1 induces patching on the cell surface, resulting in signal transduction. Disruption of GEMs inhibits cell activation (13). Thus, both the association of receptor complexes and the platform of clustered GEMs are important for signaling via the GEMs. *B3gnt5*$^{-/-}$ resting B cells showed enlarged GM1 patches on their surface, resulting in increased BCR clustering. We observed no significant differences regarding the ratio of leukocyte populations in blood between WT and *B3gnt5*$^{-/-}$ mice. However, the data at 0 min in Fig. 5 showed that phosphorylation signals were slightly up-regulated in intact *B3gnt5*$^{-/-}$ B cells, and we found that Igs in serum were slightly increased in *B3gnt5*$^{-/-}$ mice (Fig. S4). We interpret these data as implying that the clustering of GEMs containing GM1 occurred more readily in *B3gnt5*$^{-/-}$ B cells than in WT B cells. The in vivo response of B cells to TI-II antigen (TNP) was more rapid and was slightly up-regulated in *B3gnt5*$^{-/-}$ B cells as compared with WT B cells (Fig. 5*C*). This result indicated that *B3gnt5*$^{-/-}$ B cells could be activated more easily than WT B cells.

We speculated that the up-regulation of GM1 clustering caused by the absence of PLN chains from GSLs depends on structural alterations at the cell surface, such as changes in lattice structures. These structures, consisting of galectin-carbohydrate cross-linked on the cell surface, regulate signal transduction through receptor segregation and turnover, and they also modulate cellular interaction (28). Their formation on the cell surface depends on galectin binding to LacNAc (Gal) residues on glycoproteins and GSLs (28, 29). However, the formation of lattice structures is proposed to occur only via glycoprotein–glycoprotein interactions. On the other hand, Galectin-1 can bind to GM1 and 1B2–1B7-reactive GSL-containing PLN chains (30). These interactions mainly result in inhibitory effects on the diffusion of receptor molecules and small GEMs. The decreased lattice structures in *B3gnt5*$^{-/-}$ B cells may be attributable to lectin-mediated interactions of GSLs-GSLs, and/or glycoproteins-GSLs, and may cause the rapid aggregation of GEMs. In *B3gnt5*$^{-/-}$ resting B cells, the small GEMs can easily aggregate into larger units when receptor complexes are formed. Thus, B3gnt5$^{-/-}$ B cells also exhibit up-regulated phosphorylation signals and hyperproliferation, as shown in this study. Galetin-1 negatively regulates B cell proliferation and Tyr-phosphorylation on BCR stimulation (31). Marked up-regulation of galectin-1 (*Lgals1*) and galectin-3 (*Lgals3*) gene expression has been demonstrated in anergic B cells (32). These data suggest that interactions of galectins and glycans may also play a role in the regulation of immune tolerance. Dissecting the detailed mechanisms responsible for enhanced GEM formation in *B3gnt5*$^{-/-}$ B cells is an attractive subject for future study.

In addition, we observed that the behavior of BCR and BCR-related molecules was different between WT and *B3gnt5*$^{-/-}$ B cells in the GEM fraction. As seen in Fig. 4 and Fig. S7, BCR and the signaling molecule Lyn are more abundant in the GEMs of *B3gnt5*$^{-/-}$ B cells than in those of WT B cells, and thus seem to be up-regulated on translocation of these molecules into GEMs. In Fig. 4, fractions 1–4 are observed as CT-B–positive bands in both WT and *B3gnt5*$^{-/-}$ B cells. We observed that the expression pattern of BCR, CD19, and Lyn corresponds to the GEM frac-

tion, which suggests the incorporation of these molecules into GEMs. We thought that these molecules move into the GEM fractions. There is a large amount of these molecules in GEMs of *B3gnt5*$^{-/-}$ B cells stimulated with anti-CD19 Ab alone (Fig. S7). This observation also indicates that GEM-related molecules, such as BCR, CD19, and Lyn, seem to be translocated into GEMs. Alternatively, it is clear that a large amount of BCR molecules exists in the GEM fraction in *B3gnt5*$^{-/-}$ B cells as compared with WT B cells. This result reflects the state of increased ease of activation in *B3gnt5*$^{-/-}$ B cells as compared with WT B cells.

We also think that there is no possibility that expression of BCR, CD19, or Lyn was up-regulated in B cell lysates. As shown in Fig. 2, there is no difference in the cell surface expression of these molecules between WT and *B3gnt5*$^{-/-}$ B cells, as quantified by FCM analysis. In addition, Western blotting data on their presence in B cell lysates (Fig. S5) showed that the amount of these molecules did not differ between WT and *B3gnt5*$^{-/-}$ mice. However, Fig. 4 shows that the amount of BCR and/or CD19 protein in non-GEM fractions might be slightly increased. Before isolation of the GEM fraction, the lysates were separated by brief centrifugation at maximum speed to exclude nuclei and some cytoskeleton proteins, including actin. It has been reported that BCR molecules associate with certain cytoskeletal proteins; for example, cytoskeleton components, such as actin, associate with GEMs or GEM proteins, such as BCR. Actin polymerization regulates the strength of BCR stimulation (33, 34). Therefore, during this procedure, it is possible that the interaction between BCR molecules and the cytoskeleton might be affected by any alteration of GEM structure. However, we have no data to explain this difference directly at this time. In this case, it is difficult to be sure that total BCR staining is equivalent in WT and *B3gnt5*$^{-/-}$ B cells. In this study, we focused attention on the difference in the behavior of these molecules around the center or adjacent fractions of GEMs between WT and *B3gnt5*$^{-/-}$ mice.

There are at least two possible molecular mechanisms that could be responsible for the phenomenon observed in *B3gnt5*$^{-/-}$ B cells. First, BCR–CD19 complexes are transferred efficiently into GEMs, because many more clustered GEMs are formed in *B3gnt5*$^{-/-}$ B cells than in WT B cells. Second, PLN on GSLs may control the behavior of glycoprotein entry into or exclusion from GEMs. To test this hypotheses, we would need to elucidate further which molecular interactions are altered by GSL-(poly)lactosamine deficiency. The results presented here suggest that PLN on GSLs is a putative immune regulatory factor. PLN chains on GSLs may have an important role in suppression of excessive responses in the immune system in the same manner as PLN on *N*-glycans of glycoprotein. The deletion of a specific glycosyltransferase gene in knockout mice indicates that some glycosyltransferases are essential for immune system integrity. In the present study, we revealed that lacto/neolacto-series GSLs might also have significant effects on biological function in the immune system.

Experimental Procedures

Detailed information on the experimental procedures of this study, including generating *B3gnt5*-deficient mice, extraction of GSLs, glycan analysis, FCM analysis, fluorescence microscopy analysis, fractionation of GEMs, immunoblotting, cell proliferation assays, T-independent Ab production, and others, is provided in *SI Experimental Procedures and Results*. Materials, including the Abs and probes used, and glycosphingolipid structures are also described in *SI Experimental Procedures and Results*.

ACKNOWLEDGMENTS. We thank Dr. Hiroyasu Ishida of Tsukuba University and Ms. Mihou Fushimi of the National Institute of Advanced Industrial Science and Technology for excellent assistance. This work was supported by the New Energy and Industrial Technology Development Organization (NEDO).

1. Prinetti A, Loberto N, Chigorno V, Sonnino S (2009) Glycosphingolipid behaviour in complex membranes. *Biochim Biophys Acta* 1788:184–193.
2. Yohe HC, Coleman DL, Ryan JL (1985) Ganglioside alterations in stimulated murine macrophages. *Biochim Biophys Acta* 818:81–86.
3. Simons K, Ikonen E (1997) Functional rafts in cell membranes. *Nature* 387:569–572.
4. Brown DA, London E (2000) Structure and function of sphingolipid- and cholesterol-rich membrane rafts. *J Biol Chem* 275:17221–17224.
5. Hakomori S (2004) Glycosynapses: Microdomains controlling carbohydrate-dependent cell adhesion and signaling. *An Acad Bras Cienc* 76:553–572.
6. Smith DC, Lord JM, Roberts LM, Johannes L (2004) Glycosphingolipids as toxin receptors. *Semin Cell Dev Biol* 15:397–408.
7. Hakomori S (2004) Carbohydrate-to-carbohydrate interaction, through glycosynapse, as a basis of cell recognition and membrane organization. *Glycoconj J* 21:125–137.
8. Nishio M, Tajima O, Furukawa K, Urano T, Furukawa K (2005) Over-expression of GM1 enhances cell proliferation with epidermal growth factor without affecting the receptor localization in the microdomain in PC12 cells. *Int J Oncol* 26:191–199.
9. Anderson RG, Jacobson K (2002) A role for lipid shells in targeting proteins to caveolae, rafts, and other lipid domains. *Science* 296:1821–1825.
10. Petrie RJ, Schnetkamp PP, Patel KD, Awasthi-Kalia M, Deans JP (2000) Transient translocation of the B cell receptor and Src homology 2 domain-containing inositol phosphatase to lipid rafts: evidence toward a role in calcium regulation. *J Immunol* 165:1220–1227.
11. Razzaq TM, et al. (2004) Regulation of T-cell receptor signalling by membrane microdomains. *Immunology* 113:413–426.
12. Viola A, Schroeder S, Sakakibara Y, Lanzavecchia A (1999) T lymphocyte costimulation mediated by reorganization of membrane microdomains. *Science* 283:680–682.
13. Xavier R, Brennan T, Li Q, McCormack C, Seed B (1998) Membrane compartmentation is required for efficient T cell activation. *Immunity* 8:723–732.
14. Yuyama K, Sekino-Suzuki N, Sanai Y, Kasahara K (2003) Lipid rafts in cellular signaling and disease. *Trends Glycosci Glycotechnol* 15:139–151.
15. Miceli MC, et al. (2001) Co-stimulation and counter-stimulation: Lipid raft clustering controls TCR signaling and functional outcomes. *Semin Immunol* 13:115–128.
16. Togayachi A, Sato T, Narimatsu H (2006) Comprehensive enzymatic characterization of glycosyltransferases with a β3GT or β4GT motif. *Methods Enzymol* 416:91–102.
17. Togayachi A, et al. (2001) Molecular cloning and characterization of UDP-GlcNAc: lactosylceramide β1,3-*N*-acetylglucosaminyltransferase (β3Gn-T5), an essential enzyme for the expression of HNK-1 and Lewis X epitopes on glycolipids. *J Biol Chem* 276: 22032–22040.
18. Henion TR, Zhou D, Wolfer DP, Jungalwala FB, Hennet T (2001) Cloning of a mouse beta 1,3 *N*-acetylglucosaminyltransferase GlcNAc(beta 1,3)Gal(beta 1,4)Glc-ceramide synthase gene encoding the key regulator of lacto-series glycolipid biosynthesis. *J Biol Chem* 276:30261–30269.
19. Togayachi A, et al. (2007) Polylactosamine on glycoproteins influences basal levels of lymphocyte and macrophage activation. *Proc Natl Acad Sci USA* 104:15829–15834.
20. Biellmann F, Hülsmeier AJ, Zhou D, Cinelli P, Hennet T (2008) The Lc3-synthase gene B3gnt5 is essential to pre-implantation development of the murine embryo. *BMC Dev Biol* 8:109.
21. Tsubata T (1999) Co-receptors on B lymphocytes. *Curr Opin Immunol* 11:249–255.
22. Kovacic N, Müthing J, Marusic A (2000) Immunohistological and flow cytometric analysis of glycosphingolipid expression in mouse lymphoid tissues. *J Histochem Cytochem* 48: 1677–1690.
23. Schwarting GA (1980) Quantitative analysis of neutral glycosphingolipids from human lymphocyte subpopulations. *Biochem J* 189:407–412.
24. Janes PW, Ley SC, Magee AI (1999) Aggregation of lipid rafts accompanies signaling via the T cell antigen receptor. *J Cell Biol* 147:447–461.
25. Ruddock LW, et al. (1996) A pH-dependent conformational change in the B-subunit pentamer of Escherichia coli heat-labile enterotoxin: Structural basis and possible functional role for a conserved feature of the AB5 toxin family. *Biochemistry* 35: 16069–16076.
26. Pralle A, Keller P, Florin EL, Simons K, Hörber JK (2000) Sphingolipid-cholesterol rafts diffuse as small entities in the plasma membrane of mammalian cells. *J Cell Biol* 148: 997–1008.
27. Suzuki KG, Fujiwara TK, Edidin M, Kusumi A (2007) Dynamic recruitment of phospholipase C gamma at transiently immobilized GPI-anchored receptor clusters induces IP3-Ca2+ signaling: single-molecule tracking study 2. *J Cell Biol* 177:731–742.
28. Rabinovich GA, Toscano MA, Jackson SS, Vasta GR (2007) Functions of cell surface galectin-glycoprotein lattices. *Curr Opin Struct Biol* 17:513–520.
29. Garner OB, Baum LG (2008) Galectin-glycan lattices regulate cell-surface glycoprotein organization and signalling. *Biochem Soc Trans* 36:1472–1477.
30. Elola MT, Chiesa ME, Alberti AF, Mordoh J, Fink NE (2005) Galectin-1 receptors in different cell types. *J Biomed Sci* 12:13–29.
31. Yu X, Siegel R, Roeder RG (2006) Interaction of the B cell-specific transcriptional coactivator OCA-B and galectin-1 and a possible role in regulating BCR-mediated B cell proliferation. *J Biol Chem* 281:15505–15516.
32. Clark AG, et al. (2007) Multifunctional regulators of cell growth are differentially expressed in anergic murine B cells. *Mol Immunol* 44:1274–1285.
33. Brown BK, Song W (2001) The actin cytoskeleton is required for the trafficking of the B cell antigen receptor to the late endosomes. *Traffic* 2:414–427.
34. Hao S, August A (2005) Actin depolymerization transduces the strength of B cell receptor stimulation. *Mol Biol Cell* 16:2275–2284.

Enhanced humoral immune responses against T-independent antigens in Fcα/μR-deficient mice

Shin-ichiro Honda[a], Naoki Kurita[a], Akitomo Miyamoto[b], Yukiko Cho[a], Kenta Usui[a], Kie Takeshita[a], Satoru Takahashi[c], Teruhito Yasui[d], Hitoshi Kikutani[d], Taroh Kinoshita[e], Teizo Fujita[f], Satoko Tahara-Hanaoka[a], Kazuko Shibuya[a], and Akira Shibuya[a,1]

[a]Department of Immunology and [c]Anatomy and Embryology, Institute of Basic Medical Sciences, Graduate School of Comprehensive Human Sciences, and Center for TARA, University of Tsukuba, 1-1-1 Tennodai, Tsukuba, Ibaraki 305-8575, Japan; [b]Subteam for Manipulation of Cell Fate, Bioresource Center, RIKEN, 3-1-1, Koyadai, Tsukuba, Ibaraki 305-0074, Japan; Departments of [d]Molecular Immunology and [e]Immunoregulation, Research Institute of Microbial Disease, Osaka University, 3-1 Yamadaoka, Suita, Osaka 565-0871, Japan; and [f]Department of Immunology, Fukushima Medical University, 1-Hikarigaoka, Fukushima City, Fukushima 960-1295, Japan

Edited by Toshiyuki Takai, Tohoku University, Sendai, Japan, and accepted by the Editorial Board May 12, 2009 (received for review October 6, 2008)

IgM is an antibody class common to all vertebrates that plays a primary role in host defenses against infection. Binding of IgM with an antigen initiates the complement cascade, accelerating cellular and humoral immune responses. However, the functional role of the Fc receptor for IgM in such immune responses remains obscure. Here we show that mice deficient in Fcα/μR, an Fc receptor for IgM expressed on B cells and follicular dendritic cells (FDCs), have enhanced germinal center formation and affinity maturation and memory induction of IgG3$^+$ B cells after immunization with T-independent (TI) antigens. Moreover, Fcα/μR-deficient mice show prolonged antigen retention by marginal zone B (MZB) cells and FDCs. In vitro studies demonstrate that interaction of the IgM immune complex with Fcα/μR partly suppress TI antigen retention by MZB cells. We further show that downregulation of complement receptor (CR)1 and CR2 or complement deprivation by in vivo injection with anti-CR1/2 antibody or cobra venom factor attenuates antigen retention by MZB cells and germinal center formation after immunization with TI antigens in *Fcα/μR$^{-/-}$* mice. Taken together, these results suggest that Fcα/μR negatively regulates TI antigen retention by MZB cells and FDCs, leading to suppression of humoral immune responses against T-independent antigens.

Fc receptor | IgM | follicular dendritic cells (FDCs) | memory B cells | affinity maturation

IgM is an antibody class common to all vertebrates that constitutes most of the natural antibodies in the pleural and peritoneal cavities of naive hosts (1, 2). In addition, IgM is the first antibody to be produced by naive B cells upon antigen recognition. Therefore, IgM is believed to play an important role in innate immunity against variable bacterial and viral infections (3, 4). Binding of IgM with an antigen initiates the complement cascade, resulting in the acceleration of cellular and humoral immune responses (1). Mice lacking complement 3 or complement 4, or their receptors, complement receptor 1 (CR1) and complement receptor 2 (CR2) (CD35/21), show impaired IgG production in response to T-dependent (TD) antigens (5, 6). Mice lacking the secreted form of IgM (sIgM) also show markedly impaired antibody production and germinal center (GC) formation against TD antigens (7, 8). Thus IgM plays pivotal roles both in innate immunity and in the linkage between innate and adaptive immunity. However, the role of IgM in humoral immune responses against T-independent (TI) antigens is incompletely understood.

During humoral immune responses against TD antigens, an increase in GC size and number is induced in the lymphoid organs; the GC is a principal site for antibody class switching, affinity maturation, and memory B-cell generation (9–11). Follicular dendritic cells (FDCs) play a pivotal role in GC formation by retaining and presenting antigens to follicular B cells (12, 13). In contrast to TD antigens, TI antigens such as polysaccharides and glycolipids of encapsulated bacteria quickly stimulate marginal zone B (MZB) cells in the marginal zone of the follicle to produce IgM and IgG3 class antibodies (14, 15). Although antibody production against TI antigens occurs outside the follicular region, without GC formation (16), several reports have demonstrated that under certain conditions GCs are induced against TI antigens (17, 18). However, the regulation and the immunological consequences of GC formation against TI antigens remain unclear.

We previously identified an Fc receptor for IgM and IgA that we designated Fcα/μR (19, 20). The *Fcα/μR* gene has been mapped to chromosome 1 (1F in mice and 1q32.3 in humans) (19, 21) near several other Fc receptor genes, including *FcγR-I, II, III,* and *IV, FcεRI*, and the *polymeric IgR* (22–24), and Fc receptor homologues (25). Fcα/μR is expressed on the majority of follicular B cells and macrophages but not on granulocytes or T and natural killer cells. Although, unlike other immunoglobulin isotypes, IgM is present in all the vertebrate classes, Fcα/μR is the only receptor for IgM that thus far has been identified on hematopoietic cells of humans and rodents.

We show here that Fcα/μR is expressed preferentially on FDCs and MZB cells, as well as on follicular B cells, in the spleen. Interaction of IgM with Fcα/μR negatively regulates humoral immune responses against TI antigens.

Results

Increased GC Formation in Response to T-Independent Antigen in *Fcα/μR$^{-/-}$* Mice. To investigate the role of Fcα/μR in humoral immune responses in vivo, we established *Fcα/μR*-deficient (*Fcα/μR$^{-/-}$*) mice (see *SI Materials and Methods* and Fig. S1). Because Fcα/μR is expressed on B cells and FDCs (Fig. S2), we examined whether lack of Fcα/μR expression affected B-cell differentiation. Naive *Fcα/μR$^{-/-}$* mice had lymphocyte populations of normal composition in the spleen and showed no differences from their control littermates (*Fcα/μR$^{+/+}$*) in each population of B-cell subsets in the spleen, bone marrow (BM), or peritoneal cavity (data not shown), suggesting that Fcα/μR is not involved in the development of B cells or other lymphocyte lineages. We also observed no differences in the titers of each subclass of IgG and IgM in the sera of naive *Fcα/μR$^{-/-}$* mice (Fig. S3*A*).

Fcα/μR$^{-/-}$ mice demonstrated normal antibody responses

Author contributions: S.-i.H. and A.S. designed research; S.-i.H., N.K., A.M., Y.C., K.U., and K.T. performed research; N.K., S.T., T.Y., H.K., T.K., and T.F. contributed new reagents/analytic tools; S.-i.H., S.T.-H., K.S., and A.S. analyzed data; and A.S. wrote the paper.

The authors declare no conflict of interest.

This article is a PNAS Direct Submission. T.T. is a guest editor invited by the Editorial Board.

Freely available online through the PNAS open access option.

[1]To whom correspondence should be addressed. E-mail: ashibuya@md.tsukuba.ac.jp.

This article contains supporting information online at www.pnas.org/cgi/content/full/0809917106/DCSupplemental.

www.pnas.org/cgi/doi/10.1073/pnas.0809917106

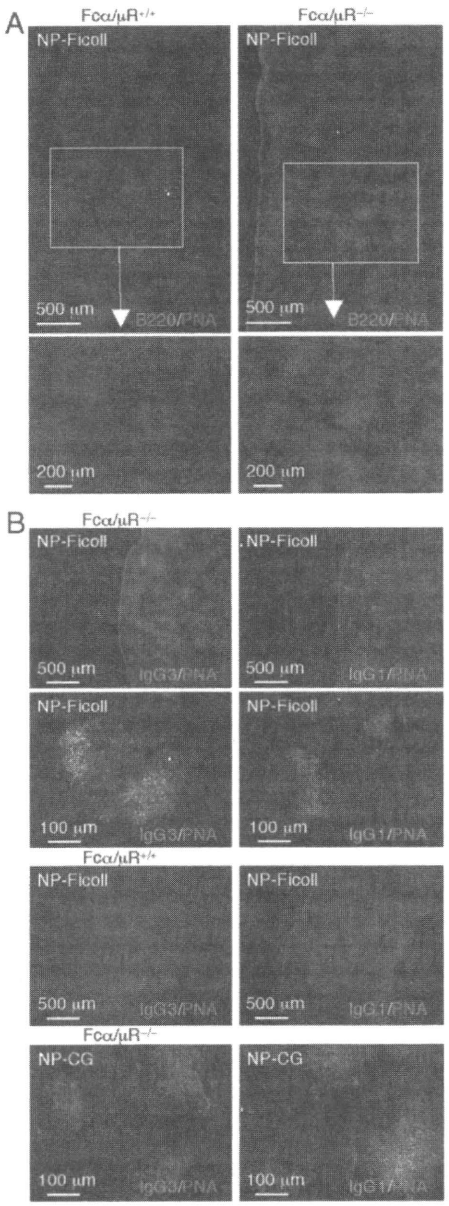

Fig. 1. GC reaction against T-independent (TI) antigens in $Fc\alpha/\mu R^{-/-}$ mice. $Fc\alpha/\mu R^{+/+}$ or $Fc\alpha/\mu R^{-/-}$ mice were immunized i.p. with the TD antigen (NP-CG) emulsified with alum or with the TI antigen NP-Ficoll. A week (for NP-Ficoll) or 2 weeks (for NP-CG) after the immunization, spleen sections were stained with biotinylated PNA, followed by Alexa594-conjugated streptavidin and FITC-conjugated anti-B220 (*A*) or with anti-mouse IgG3 or IgG1 (*B*). Data are representative of 3 independent experiments.

after immunization with the TD antigen 4-hydroxy-3-nitrophenylacetyl-chicken gamma globulin (NP-CG), the TI type 1 antigen NP-LPS, or the TI type 2 antigen NP-Ficoll (Fig. S3*B*). Unexpectedly, however, immunization with either of the TI antigens significantly increased the number and size of GCs in the spleen in $Fc\alpha/\mu R^{-/-}$mice but not $Fc\alpha/\mu R^{+/+}$ mice (Fig. 1*A* and data not shown). Although these GCs were Bcl-6^{+}, $B220^{dull}$, and IgD^{low}, similar to those induced after immunization with TD antigens (data not shown), they preferentially produced IgG3 (Fig. 1*B*), rather than the IgG1 detected in the GC B cells induced by the TD antigen NP-CG. Analyses by flow cytometry showed that the numbers of GC B cells, defined as $B220^{+}$, $GL7^{+}$ cells (26), increased significantly in $Fc\alpha/\mu R^{-/-}$ mice after immunization with the TI antigens NP-Ficoll and NP-LPS but not after immunization with the TD antigen NP-CG (Fig. 2*A* and Table S1). Similar results were obtained by flow cytometry when GC B cells were defined more specifically as PNA^{high}, $GL7^{+}$ cells (Fig. 2*B*). Depletion of $CD4^{+}$ T cells by in vivo injection of an anti-CD4 monoclonal antibody diminished the number of GC B cells after immunization with NP-CG but not after immunization with NP-Ficoll in both $Fc\alpha/\mu R^{-/-}$ and $Fc\alpha/\mu R^{+/+}$ mice (Fig. 2*A*), demonstrating that the increased GC reaction to NP-Ficoll in $Fc\alpha/\mu R^{-/-}$ mice was a T-cell-independent event.

To determine the cell types expressing Fcα/μR responsible for the increased GC formation in response to TI antigens in $Fc\alpha/\mu R^{-/-}$ mice, we established BM chimeric $Fc\alpha/\mu R^{+/+}$ or $Fc\alpha/\mu R^{-/-}$ mice reconstituted with either $Fc\alpha/\mu R^{+/+}$ or $Fc\alpha/\mu R^{-/-}$ BM cells. Because FDCs are radio resistant and therefore are not replaced by donor cells following BM transfer (27), these BM chimeric mice would have donor-derived B cells and recipient-derived FDCs. Immunization with NP-Ficoll increased the number of GC B cells in both $Fc\alpha/\mu R^{+/+}$ and $Fc\alpha/\mu R^{-/-}$ mice reconstituted with $Fc\alpha/\mu R^{-/-}$ and $Fc\alpha/\mu R^{+/+}$ BM cells, respectively, to a significantly greater degree than in $Fc\alpha/\mu R^{+/+}$ mice reconstituted with $Fc\alpha/\mu R^{+/+}$ BM cells (Fig. 2*C*). These results suggest that lack of Fcα/μR expression on both FDCs and B cells is responsible for the enhanced GC formation in response to TI antigens.

Generation of Memory B Cells in Response to TI Antigens in $Fc\alpha/\mu R^{-/-}$ Mice. We then examined whether enhanced GC formation led to memory B-cell generation after immunization with TI antigens in $Fc\alpha/\mu R^{-/-}$ mice. $Fc\alpha/\mu R^{-/-}$ and $Fc\alpha/\mu R^{+/+}$ mice were immunized with NP-Ficoll and were re-challenged with the same antigen 12 weeks after the first immunization. Although the antibody titers again increased in both $Fc\alpha/\mu R^{-/-}$ and $Fc\alpha/\mu R^{+/+}$ mice 1 week after the second immunization, they did not exceed those at 1 week after the first immunization in either group of mice (Fig. S4). These results suggest that memory B cells specific to NP-Ficoll had not been generated. However, it also was possible that the large amount of anti-NP IgG3 that was still detectable in the sera of both groups of mice before the second immunization and that might have been produced by long-lived plasma cells was veiling a small recall response by memory B cells in response to NP-Ficoll.

To dissect further the antibody responses by memory B cells to the second immunization, spleen cells or BM cells from $Fc\alpha/\mu R^{-/-}$ and $Fc\alpha/\mu R^{+/+}$ mice before or 7 weeks after immunization with NP-Ficoll were transferred into SCID mice, which then were challenged with the same antigen on the following day (Fig. 3*A*). A week after the immunization, NP-specific IgG3 production in the SCID mice that had been given the $Fc\alpha/\mu R^{-/-}$ BM cells was significantly greater than that in the SCID mice given the $Fc\alpha/\mu R^{+/+}$ BM cells (Fig. 3*B*). We barely detected NP-specific IgG1 in either group of SCID mice (Fig. 3*B*). In contrast, we did not observe any difference in NP-specific IgG3 production between SCID mice transferred with spleen cells from $Fc\alpha/\mu R^{-/-}$ and $Fc\alpha/\mu R^{+/+}$ mice (data not shown). Because NP-specific IgG3 was not detected in SCID mice that received BM cells from primed mice without the second immunization (Fig. 3*B*), long-lived plasma cells may absent or very rare in BM cells. Collectively, these results suggest that enhanced GC formation in response to TI antigens in $Fc\alpha/\mu R^{-/-}$ mice led to the generation of memory B cells producing IgG3.

Affinity Maturation of $IgG3^{+}$ B Cells Specific to TI Antigens in $Fc\alpha/\mu R^{-/-}$ Mice. We next examined whether increased GC formation also was associated with affinity maturation of B cells in $Fc\alpha/\mu R^{-/-}$ mice. $Fc\alpha/\mu R^{-/-}$ mice and $Fc\alpha/\mu R^{+/+}$ mice were

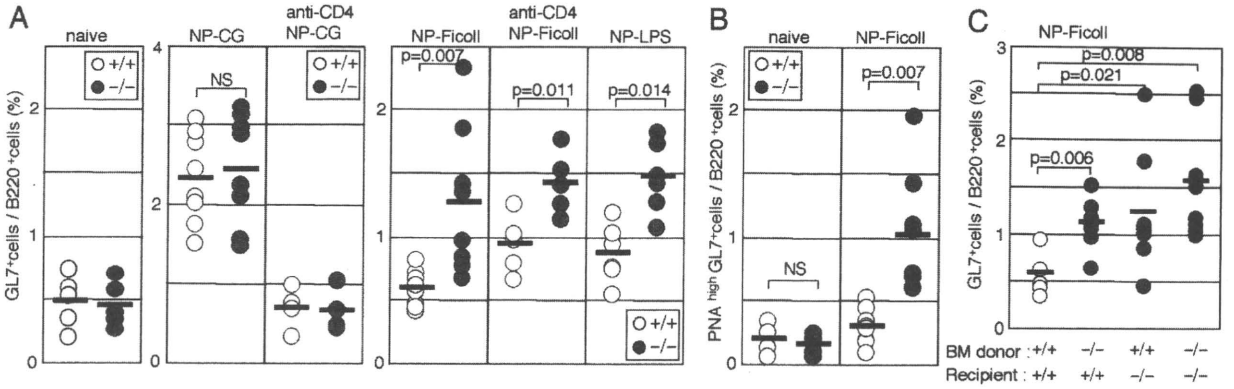

Fig. 2. GC B cells after immunization with T-dependent (TD) or T-independent (TI) antigens in $Fc\alpha/\mu R^{-/-}$ mice. (*A*, *B*) $Fc\alpha/\mu R^{+/+}$ or $Fc\alpha/\mu R^{-/-}$ mice (n = 5–9) were immunized i.p. with TD antigen (NP-CG) emulsified with alum or with TI antigens NP-Ficoll or NP-LPS. A week (for NP-Ficoll and NP-LPS) or 2 weeks (for NP-CG) after the immunization, spleen cells were stained with FITC-conjugated anti-GL-7 and PE-conjugated anti-B220 (*A*) or biotinylated PNA, followed by APC-conjugated streptavidin (*B*). To deplete $CD4^+$ T cells, mice were injected with anti-CD4 (GK1.5) mAb before immunization. Data are representative of 3 independent experiments. (*C*) We injected 5×10^6 BM cells from $Fc\alpha/\mu R^{+/+}$ or $Fc\alpha/\mu R^{-/-}$ mice via the tail vein into lethally irradiated $Fc\alpha/\mu R^{+/+}$ or $Fc\alpha/\mu R^{-/-}$ mice (n = 6–8/group). BM chimeric mice were immunized with NP-Ficoll 6 to 8 weeks later, and $GL7^+$ cells among $B220^+$ cells in the spleen were analyzed 1 week after immunization, as described previously. Data are representative of 2 independent experiments.

immunized with NP-Ficoll or NP-LPS and then were re-challenged with the same antigens 12 weeks later. Sera were collected 1 week and 12 weeks after the first antigen challenges and 1 week after the second antigen challenges and were measured for affinity of NP-specific antibody (Fig. 4*A*). The affinity for NP-specific IgG3 was comparable between $Fc\alpha/\mu R^{-/-}$ and $Fc\alpha/\mu R^{+/+}$ mice 1 week and 12 weeks after the first antigen challenges (data not shown). Although in $Fc\alpha/\mu R^{+/+}$ mice the affinity for NP-specific IgG3 after the second immunization was comparable to that after the first immunization, $Fc\alpha/\mu R^{-/-}$ mice showed significantly higher affinity for NP-specific IgG3 after the second immunization than after the first immunization (Fig. 4*B* and Fig. S5). In contrast, affinities for NP-specific IgG1 were low after the first immunization and were not altered after the second antigen challenge in both $Fc\alpha/\mu R^{-/-}$ and $Fc\alpha/\mu R^{+/+}$ mice (Fig. 4*B* and Fig. S5). These results indicate that $Fc\alpha/\mu R^{-/-}$ mice showed affinity maturation of NP-specific IgG3 after the second challenge with the TI antigens NP-Ficoll or NP-LPS.

To elucidate the molecular basis of the affinity maturation in $Fc\alpha/\mu R^{-/-}$ mice, we examined whether NP-Ficoll induced somatic hypermutation (SHM) in NP-specific $V_H186.2$ $IgG3^+$ B cells in $Fc\alpha/\mu R^{-/-}$ mice. $Fc\alpha/\mu R^{-/-}$ and $Fc\alpha/\mu R^{+/+}$ mice were immunized with NP-Ficoll; then PCR was performed to amplify $V_H186.2$ IgG3 clones from the spleen. We analyzed more than 10 amplified clones and barely detected the $V_H186.2$ clone from the spleen of naive $Fc\alpha/\mu R^{-/-}$ and $Fc\alpha/\mu R^{+/+}$ mice. However, more than half the clones amplified from $Fc\alpha/\mu R^{-/-}$ and $Fc\alpha/\mu R^{+/+}$ mice 1 week after immunization were $V_H186.2$ clones, suggesting that the $V_H186.2$ clone was expanded in response to the immunization. We observed only a few mutations in the $V_H186.2$ clones from $Fc\alpha/\mu R^{-/-}$ and $Fc\alpha/\mu R^{+/+}$ mice 1 week after immunization (Fig. S6). However, in recall responses, $Fc\alpha/\mu R^{-/-}$ mice had higher frequencies of SHM in

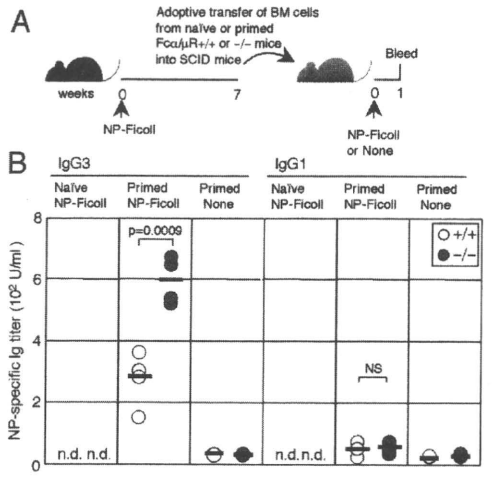

Fig. 3. Recall response against TI antigen in $Fc\alpha/\mu R^{-/-}$ mice. (*A*) $Fc\alpha/\mu R^{+/+}$ or $Fc\alpha/\mu R^{-/-}$ mice were immunized with NP-Ficoll or were not immunized (naive mice). BM cells from naive mice or from the $Fc\alpha/\mu R^{+/+}$ or $Fc\alpha/\mu R^{-/-}$ mice primed with NP-Ficoll were transferred to SCID mice 7 weeks after immunization. The SCID mice then were re-challenged with the same antigen or were not re-challenged. (*B*) Anti-NP IgG3 or IgG1 titers in SCID mice were determined 1 week after the second challenge. n.d., not detected.

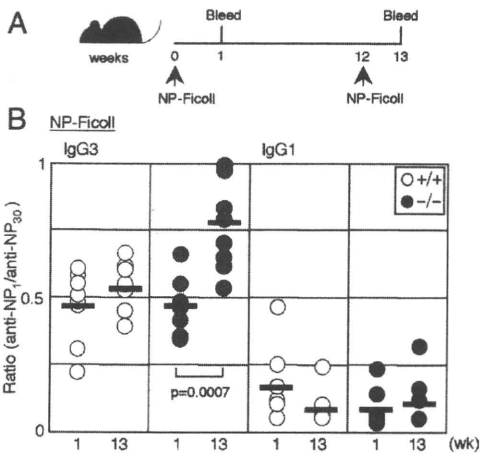

Fig. 4. Affinity maturation after immunization with TI antigen in $Fc\alpha/\mu R^{-/-}$ mice. (*A*) $Fc\alpha/\mu R^{+/+}$ or $Fc\alpha/\mu R^{-/-}$ mice were immunized with NP-Ficoll and were re-challenged with the same antigen 12 weeks later. (*B*) The affinities of anti-NP IgG3 and IgG1 in the sera were determined 1 week after the first immunization and after the second immunization, as described in the experimental procedures.

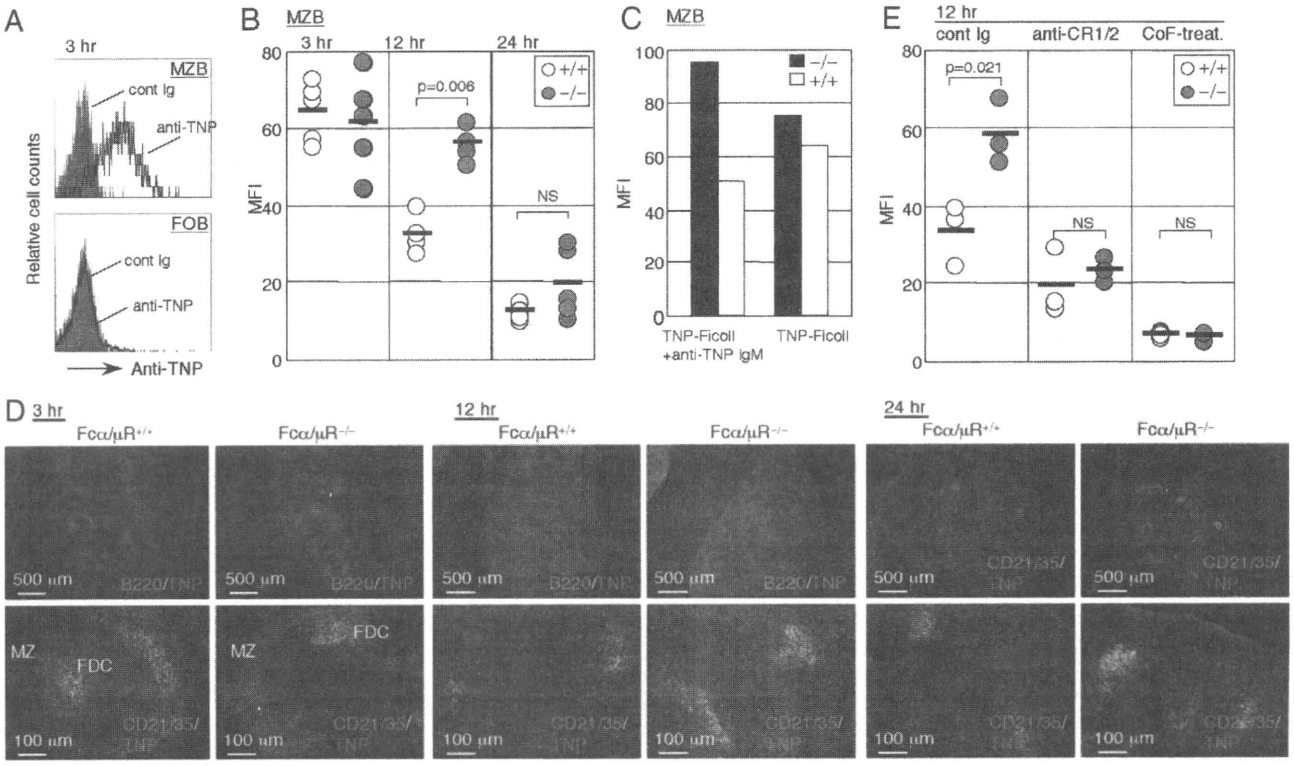

Fig. 5. TI antigen retention on MZB cells and FDCs in $Fc\alpha/\mu R^{-/-}$ mice. (*A*, *B*) $Fc\alpha/\mu R^{+/+}$ or $Fc\alpha/\mu R^{-/-}$ mice were injected i.v. with 50 μg of TNP-Ficoll. Spleen cells were stained with biotin-conjugated anti-TNP, followed by APC-conjugated streptavidin, FITC-conjugated anti-CD21/35, and PE-conjugated anti-CD23 3, 12, or 24 hours after injection. (*A*) Representative flow cytometry profiles of TNP signal on MZB cells ($CD21/35^{high}$, $CD23^{-}$) and FOB cells ($CD21/35^{+}$, $CD23^{+}$) are shown. (*B*) The mean fluorescence intensity (MFI) of the TNP signal on MZB cells is shown. (*C*) Spleen cells from $Fc\alpha/\mu R^{+/+}$ or $Fc\alpha/\mu R^{-/-}$ mice were incubated with TNP-Ficoll alone or with anti-TNP IgM (IgM IC) in the presence of *RAG*-deficient mouse serum. Cells were stained with biotin-conjugated anti-TNP, followed by APC-conjugated streptavidin, FITC-conjugated anti-CD21/35, and PE-conjugated anti-CD23 for flow cytometry analysis. The MFI of TNP signals on MZB- and FOB-gated cells is shown. (*D*) After antigen injection, the spleen sections were stained with biotin-conjugated anti-TNP, followed by Alexa 594-conjugated streptavidin and FITC-conjugated anti-CD21/35 or anti-B220. (*E*) $Fc\alpha/\mu R^{+/+}$ or $Fc\alpha/\mu R^{-/-}$ mice were injected i.v. with anti-CR1/2, control antibody, or CoF before immunization with TNP-Ficoll. Spleen cells were stained with biotin-conjugated anti-TNP 12 hours after the immunization, followed by APC-conjugated streptavidin, FITC-conjugated anti-CD1d, and PE-conjugated anti-CD23. The MFI of TNP signal on MZB-gated cells ($CD1d^{high}$, $CD23^{-}$) is shown.

the V_H genes of anti-NP IgG3 than did $Fc\alpha/\mu R^{+/+}$ mice (Fig. S6). These increased SHM might cause affinity maturation of NP-specific IgG3 in $Fc\alpha/\mu R^{-/-}$ mice.

Prolongation of TI Antigen Retention on MZB Cells and FDCs in $Fc\alpha/\mu R^{-/-}$ Mice. Our next goal was to determine how Fcα/μR expressed on FDCs and B cells is involved in GC formation. Because MZB cells and FDCs capture antigens efficiently, we speculated that Fcα/μR was involved in TI antigen retention on MZB cells and/or FDCs. To test this hypothesis, we injected 2,4,6-trinitrophenyl (TNP)-Ficoll i.v. into $Fc\alpha/\mu R^{-/-}$ or $Fc\alpha/\mu R^{+/+}$ mice and analyzed antigen retention by using anti-TNP antibody. In both $Fc\alpha/\mu R^{-/-}$ mice and $Fc\alpha/\mu R^{+/+}$ mice, flow cytometry analyses detected the TNP signal on MZB cells ($CD21/35^{high}$, $CD23^{-}$ cells) but not on follicular B (FOB) cells ($CD21/35^{+}$, $CD23^{+}$ cells) 3 hours after TNP-Ficoll injection (Fig. 5*A* and data not shown). The extent of antigen retention on MZB cells, as determined by the intensity of the TNP signals, was comparable in $Fc\alpha/\mu R^{-/-}$ mice and $Fc\alpha/\mu R^{+/+}$ mice 3 hours after antigen injection. Although the TNP signal on MZB cells gradually declined with time, its diminution was much slower in $Fc\alpha/\mu R^{-/-}$ mice than in $Fc\alpha/\mu R^{+/+}$ mice (Fig. 5*B*).

To examine whether IgM is involved in TI antigen retention by MZB cells, we incubated MZB cells derived from $Fc\alpha/\mu R^{-/-}$ mice and $Fc\alpha/\mu R^{+/+}$ mice with either TNP-Ficoll alone or an immune complex (IC) of TNP-Ficoll and anti-TNP IgM in a culture medium containing sera from $RAG^{-/-}$ mice (the medium contained complement but not IgM antibody) and analyzed antigen binding by flow cytometry using anti-TNP antibody. TNP-Ficoll retention (as determined from the mean fluorescence intensity of anti-TNP antibody) by $Fc\alpha/\mu R^{-/-}$ cells and $Fc\alpha/\mu R^{+/+}$ MZB cells in the absence of anti-TNP IgM was comparable, but the $Fc\alpha/\mu R^{-/-}$ MZB cells captured the IgM IC to a greater degree than did the $Fc\alpha/\mu R^{+/+}$ MZB cells (Fig. 5*C*). In contrast, antigen retention was not observed, even in the presence of anti-TNP IgM, on either $Fc\alpha/\mu R^{-/-}$ or $Fc\alpha/\mu R^{+/+}$ FOB cells (data not shown). These results indicated that the interaction of Fcα/μR with IgM IC inhibited TI antigen retention by MZB cells.

Immunohistochemical analyses showed that the antigen was preferentially localized in the marginal zone area 3 hours after antigen injection in both $Fc\alpha/\mu R^{-/-}$ and $Fc\alpha/\mu R^{+/+}$ mice (Fig. 5*D*). Notably, the TNP signal also was detected on FDCs in the follicles in both $Fc\alpha/\mu R^{-/-}$ and $Fc\alpha/\mu R^{+/+}$ mice (Fig. 5*D*), suggesting that TNP-Ficoll is captured by the FDCs as early as 3 hours after antigen injection. Although 12 hours after antigen injection the TNP signal was scarcely detected in the marginal zone area in both $Fc\alpha/\mu R^{-/-}$ and $Fc\alpha/\mu R^{+/+}$ mice and on the FDCs of $Fc\alpha/\mu R^{+/+}$ mice, it still was readily detectable on the FDCs of $Fc\alpha/\mu R^{-/-}$ mice (Fig. 5*D*). These results indicate that the retention of TI antigen on MZB cells and FDCs is prolonged in $Fc\alpha/\mu R^{-/-}$ mice.

Involvement of the Complement Pathway in Humoral Immune Responses against TI Antigens in $Fc\alpha/\mu R^{-/-}$ Mice. Previous reports have demonstrated that humoral immune responses against TI antigens are defective in the absence of complement (28, 29). To determine whether the complement pathway is involved in the increased humoral immune response against TI antigens in $Fc\alpha/\mu R^{-/-}$ mice, we injected $Fc\alpha/\mu R^{-/-}$ and $Fc\alpha/\mu R^{+/+}$ mice with the anti-CR1/2 monoclonal antibody 7G6, which is able to downmodulate the expression of CR1 and CR2 (CD35/21) (30). These mice were injected with the TI antigen TNP-Ficoll 2 days later. Flow cytometric analyses showed that, 12 hours after the antigen injection, antigen retention on the MZB cells of $Fc\alpha/\mu R^{-/-}$ mice had returned to the level in $Fc\alpha/\mu R^{+/+}$ mice (Fig. 5*E*). Because antigen retention by MZB cells is associated with GC formation, we next examined whether the presence of 7G6 antibody also affected GC formation in $Fc\alpha/\mu R^{-/-}$ mice. $Fc\alpha/\mu R^{-/-}$ and $Fc\alpha/\mu R^{+/+}$ mice were immunized with NP-Ficoll 2 days after injection with 7G6 antibody. A week after the immunization, flow cytometric analyses demonstrated that the number of GC B cells in the spleen of $Fc\alpha/\mu R^{-/-}$ mice had returned to the level in $Fc\alpha/\mu R^{+/+}$ mice (Fig. S7*A*). Supporting these results, complement deprivation by injection with cobra venom factor (CoF) attenuated antigen retention and GC formation in response to TI antigens in $Fc\alpha/\mu R^{-/-}$ mice (Fig. 5*E* and Fig. S7*A*). Moreover, the reduction of GC formation by CoF in $Fc\alpha/\mu R^{-/-}$ mice resulted in the diminution of affinity maturation of IgG3 antibody (Fig. S7*B*). Taken together, these results suggest that the increased antigen retention on MZB cells and enhanced GC formation in $Fc\alpha/\mu R^{-/-}$ mice depends on CR1/2.

Discussion

Our results represent the characterization of mice deficient in Fcα/μR. We demonstrated that TI antigens induce enhanced GC formation (Figs. 1 and 2), IgG3 memory response (Fig. 3), and affinity maturation (Fig. 4) in $Fc\alpha/\mu R^{-/-}$ mice. In contrast, we observed no differences between $Fc\alpha/\mu R^{+/+}$ mice and $Fc\alpha/\mu R^{-/-}$ mice in humoral immune response against TD antigens. Although an increase in GC number and size obviously is induced in response to TD antigens (9–11), several lines of evidence have demonstrated that GCs also can be induced against TI antigens, although the response is not as marked as the response to TD antigens (17, 18). However, the structural and functional characteristics of TI antigen-induced GCs have not been elucidated. Although GC reaction was enhanced in $Fc\alpha/\mu R^{-/-}$ mice after immunization with TI antigens, antibody titers in the sera were not elevated, an observation that is in line with previous findings (31). Instead, we observed increased SHM in the V_H genes of IgG3 and affinity maturation of IgG3 against NP-conjugated TI antigens in $Fc\alpha/\mu R^{-/-}$ mice (Fig. S6), consistent with previous reports that SHM occurs within GCs, albeit at low levels, in response to TI antigens (18, 32). We observed increased SHM of anti-NP IgG3 in $Fc\alpha/\mu R^{-/-}$ mice, and this increase might have been associated with affinity maturation of IgG3 after the second challenge by TI antigens. Moreover, we showed that BM cells from $Fc\alpha/\mu R^{-/-}$ mice (but not from $Fc\alpha/\mu R^{+/+}$ mice) primed with TI antigens produced enhanced amounts of anti-NP IgG3 in SCID mice in response to the second antigen challenge (Fig. 3). We indeed detected IgG3, rather than IgG1, localized within enlarged GC areas after immunization with NP-Ficoll (Fig. 1*B*). These results collectively suggest that memory B cells that produced high-affinity IgG3 specific to TI antigens were generated as part of the enhanced GC formation in response to TI antigens in $Fc\alpha/\mu R^{-/-}$ mice.

We also demonstrated prolonged retention of TI antigen on MZB cells and FDCs in $Fc\alpha/\mu R^{-/-}$ mice (Fig. 5). Retention of TI antigens by MZB cells is diminished in complement 3-deficient mice (28, 33), indicating that this process is complement dependent. Here, we found that modulation of complement receptor expression by in vivo injection with anti-CR1/2 antibody or complement deprivation by CoF injection abrogated the TI antigen retention on MZB cells in both $Fc\alpha/\mu R^{-/-}$ and $Fc\alpha/\mu R^{+/+}$ mice (Fig. 5*E*). Moreover, this modulation also diminished the number of GC cells produced in response to TI antigens in $Fc\alpha/\mu R^{-/-}$ mice (Fig. S7*A*). Collectively, these results indicate that increased complement-dependent TI antigen retention on MZB cells leads to enhanced GC reaction in response to TI antigens in $Fc\alpha/\mu R^{-/-}$ mice.

Because the *SLAM* gene, which maps closely to the $Fc\alpha/\mu$R on chromosome 1, has been shown to affect lymphocyte activity in mice of the 129 strain (34), it is possible that the phenotype observed in the $Fc\alpha/\mu R^{-/-}$ mice might result from the remaining *SLAM* gene derived from E14 ES cells with the 129 genetic background. To address this issue, we subsequently established a new line of $Fc\alpha/\mu R^{-/-}$ mice by using BALB/c ES cells (Fig. S8 *A* and *B*). We also observed increased GC formation and antigen retention on MZB cells and FDCs after TI-antigen challenge in BALB/c Fcα/μR-deficient mice (Fig. S8 *C–F*). Thus, we concluded that the phenotype in the Fcα/μR-deficient mice of B6/129 background resulted from the deficiency of Fcα/μR.

An important question that has remained unanswered is the molecular mechanism of the functional association of the complement cascade with Fcα/μR. Our data suggest that Fcα/μR negatively regulates CR1/2-mediated antigen retention by MZB cells. The classic complement cascade is initiated by C1q binding to the Fc portion of IgM bound to an antigen (35). Therefore, a simple explanation would be that the binding of IgM IC to Fcα/μR prevents C1q from binding to the Fc portion of IgM of the IC, resulting in downregulation of the complement cascade on MZB cells. However, this scenario seemed unlikely, because we did not observe such competition between Fcα/μR and C1q for binding to the Fc portion of IgM in IC (data not shown). Another hypothesis that could explain the Fcα/μR-mediated negative regulation of complement-dependent antigen retention by MZB cells is that Fcα/μR and CR1/2 compete for IgM- or complement-mediated binding of antigen to each receptor. An alternative explanation would be that interaction of IgM IC with Fcα/μR mediates signals that affect CR1/2 function in complement binding. In the present study, we also showed that antigen retention is prolonged on FDCs that markedly express both Fcα/μR and CR1/2 (Fig. 5*D*). Therefore, it also is essential that we clarify whether and how Fcα/μR suppresses CR1/2-mediated antigen retention by FDCs. Further analyses are required to determine the molecular and functional association between Fcα/μR and CR1/2 on MZB cells and FDCs.

We demonstrated that the interaction of IgM with Fcα/μR is primarily involved in antigen retention in vitro (Fig. 5*C*). Therefore, mice deficient in sIgM might be similar to $Fc\alpha/\mu R^{-/-}$ mice. In fact, sIgM-deficient mice show increased IgG2a and IgG2b (7) or IgG3 (8) production in response to NP-Ficoll. We observed increased IgG3 production after the second NP-Ficoll challenge in $Fc\alpha/\mu R^{-/-}$ mice, which demonstrated a phenotype similar to that of sIgM mice in the context of enhanced humoral immune responses against TI antigens. On the other hand, sIgM-deficient mice also show markedly impaired antibody production and GC formation in response to TD antigens (7, 8) that was not observed in $Fc\alpha/\mu R^{-/-}$ mice, suggesting that IgM acts not only as a ligand for Fcα/μR but also has other important roles in the immune response. Of note, mice deficient in sIgM show accelerated development of IgG autoantibodies and autoimmune diseases (36, 37). These results suggest that interaction of the IgM immune complex with Fcα/μR suppresses the humoral immune response against self-antigens. Because most natural antibodies are polyreactive to TI antigens, including a variety of foreign antigens and self-antigens (1, 38), our results shed light on humoral immune responses against both infections and self-antigens.

Materials and Methods

Materials and methods for mice, antibodies, ELISA, immunohistochemistry, generation of BM chimeric mice, and the SHM assay used here are described in *SI Materials and Methods*.

Immunization. For every immunization, wild-type ($Fc\alpha/\mu R^{+/+}$) littermate mice were used as controls for $Fc\alpha/\mu R^{-/-}$ mice. $Fc\alpha/\mu R^{-/-}$ and $Fc\alpha/\mu R^{+/+}$ mice (8 to 12 weeks old) were immunized i.p. with 10 μg NP-CG emulsified with alum as a TD antigen. For TI antigen immunization, 10 μg NP-Ficoll or NP-LPS (Biosearch Technologies) was injected i.p. For recall response, mice were rechallenged with either TI antigen 12 weeks after primary immunization. Sera were collected 1 week after each immunization and were used for ELISA analysis. For in vivo depletion of CD4 T cells, mice were given 100 μg of anti-CD4 (GK1.5) mAb i.p. 2 days before immunization. For downmodulation of CR1/2 in vivo, mice were given 200 μg anti-CR1/2 (7G6) mAb i.p. 2 days before immunization. For complement depletion, 3 μg of CoF was injected into each mouse via the tail vein 1 day before immunization. For the BM cell transfer experiment, 2×10^7 BM cells obtained from $Fc\alpha/\mu R^{-/-}$ or $Fc\alpha/\mu R^{+/+}$ mice 7 weeks after NP-Ficoll immunization were transferred into CB17.SCID mice that were immunized with the same antigen 1 day later.

Affinity Measurement. Antibody affinity was measured by using plates coated with either NP_{30}-BSA or NP_1-BSA. Sera were diluted serially to determine the dilution multitude to the absorbance 2 times greater than background, by using HRP-conjugated goat Abs specific for each mouse immunoglobulin isotype. The ratios of dilution multitudes determined by each plate coated by NP_{30}-BSA or NP_1-BSA were calculated for individual sera.

Antigen Retention Analysis. Mice were injected with 50 μg of TNP-Ficoll (Biosearch) via the tail vein. The splenocytes then were stained with biotin-conjugated hamster anti-TNP IgG, followed by allophycocyanin (APC)-conjugated streptavidin in combination with FITC-conjugated anti-CD21/35 and phycoerythrin (PE)-conjugated anti-CD23 (PharMingen) for flow cytometric analyses. For immunohistochemical analyses, frozen sections of the spleen were incubated with biotin-conjugated hamster anti-TNP IgG (PharMingen), followed by Alexa 594-conjugated streptavidin (Invitrogen) in combination with FITC-conjugated anti-CD21/35 or anti-B220. For the in vitro experiment, TNP-Ficoll was incubated with anti-TNP mouse IgM (PharMingen) for 30 min at 37 °C and then cultured for 15 min at 37 °C with splenocytes in 1% $RAG^{-/-}$ mouse-derived serum containing TC buffer [140 mM NaCl, 2 mM $CaCl_2$, 2 mM $MgCl_2$, 10 mM Tris (pH 7.5), supplemented with 1% BSA]. The cells were stained for flow cytometric analysis as described earlier in the article.

Statistics. Statistical analyses were performed by using Student's unpaired *t* test.

ACKNOWLEDGMENTS. We thank L. Lanier and J. Cyster for critical reading of this manuscript and Y. Soeda for secretarial assistance. This research was supported in part by grants provided by the Ministry of Education, Science, and Culture of Japan; Special Coordination Funds from the Science and Technology Agency of the Japanese Government; the Program for Promotion of Fundamental Studies in Health Science of the National Institute of Biomedical Innovation (NIBIO); and the Uehara Memorial Foundation.

1. Ochsenbein AF, Zinkernagel RM (2000) Natural antibodies and complement link innate and acquired immunity. *Immunol Today* 21(12):624–630.
2. Casali P, Schettino EW (1996) Structure and function of natural antibodies. *Curr Top Microbiol Immunol* 210:167–179.
3. Ochsenbein AF, et al. (1999) Control of early viral and bacterial distribution and disease by natural antibodies. *Science* 286(5447):2156–2159.
4. Boes M, Prodeus AP, Schmidt T, Carroll MC, Chen J (1998) A critical role of natural immunoglobulin M in immediate defense against systemic bacterial infection. *J Exp Med* 188(12):2381–2386.
5. Carroll MC (2004) The complement system in regulation of adaptive immunity. *Nat Immunol* 5(10):981–986.
6. Fischer MB, et al. (1996) Regulation of the B cell response to T-dependent antigens by classical pathway complement. *J Immunol* 157(2):549–556.
7. Boes M, et al. (1998) Enhanced B-1 cell development, but impaired IgG antibody responses in mice deficient in secreted IgM. *J Immunol* 160(10):4776–4787.
8. Ehrenstein MR, O'Keefe TL, Davies SL, Neuberger MS (1998) Targeted gene disruption reveals a role for natural secretory IgM in the maturation of the primary immune response. *Proc Natl Acad Sci USA* 95(17):10089–10093.
9. Kelsoe G (1996) Life and death in germinal centers (redux). *Immunity* 4(2):107–111.
10. MacLennan IC (2005) Germinal centers still hold secrets. *Immunity* 22(6):656–657.
11. Manser T (2004) Textbook germinal centers? *J Immunol* 172(6):3369–3375.
12. Park CS, Choi YS (2005) How do follicular dendritic cells interact intimately with B cells in the germinal centre? *Immunology* 114(1):2–10.
13. Chaplin DD, Zindl CL (2006) Taking control of follicular dendritic cells. *Immunity* 24(1):13–15.
14. Martin F, Kearney JF (2002) Marginal-zone B cells. *Nature Reviews Immunology* 2(5):323–335.
15. Lopes-Carvalho T, Kearney JF (2004) Development and selection of marginal zone B cells. *Immunol Rev* 197:192–205.
16. MacLennan IC, et al. (2003) Extrafollicular antibody responses. *Immunol Rev* 194:8–18.
17. de Vinuesa CG, et al. (2000) Germinal centers without T cells. *J Exp Med* 191(3):485–494.
18. Lentz VM, Manser T (2001) Cutting edge: Germinal centers can be induced in the absence of T cells. *J Immunol* 167(1):15–20.
19. Shibuya A, et al. (2000) Fc alpha/mu receptor mediates endocytosis of IgM-coated microbes. *Nat Immunol* 1(5):441–446.
20. Sakamoto N, et al. (2001) A novel Fc receptor for IgA and IgM is expressed on both hematopoietic and non-hematopoietic tissues. *Eur J Immunol* 31(5):1310–1316.
21. Shimizu Y, et al. (2001) Fc(alpha)/mu receptor is a single gene-family member closely related to polymeric immunoglobulin receptor encoded on chromosome 1. *Immunogenetics* 53(8):709–711.
22. Daeron M (1997) Fc receptor biology. *Annu Rev Immunol* 15:203–234.
23. Ravetch JV, Bolland S (2001) IgG Fc receptors. *Annu Rev Immunol* 19:275–290.
24. Nimmerjahn F, Ravetch JV (2006) Fcgamma receptors: Old friends and new family members. *Immunity* 24(1):19–28.
25. Davis RS, Wang YH, Kubagawa H, Cooper MD (2001) Identification of a family of Fc receptor homologs with preferential B cell expression. *Proc Natl Acad Sci USA* 98(17):9772–9777.
26. Takahashi Y, Dutta PR, Cerasoli DM, Kelsoe G (1998) In situ studies of the primary immune response to (4-hydroxy-3-nitrophenyl)acetyl. V. Affinity maturation develops in two stages of clonal selection. *J Exp Med* 187(6):885–895.
27. Ahearn JM, et al. (1996) Disruption of the Cr2 locus results in a reduction in B-1a cells and in an impaired B cell response to T-dependent antigen. *Immunity* 4(3):251–262.
28. Guinamard R, Okigaki M, Schlessinger J, Ravetch JV (2000) Absence of marginal zone B cells in Pyk-2-deficient mice defines their role in the humoral response. *Nat Immunol* 1(1):31–36.
29. Fearon DT, Carroll MC (2000) Regulation of B lymphocyte responses to foreign and self-antigens by the CD19/CD21 complex. *Annu Rev Immunol* 18:393–422.
30. Thyphronitis G, et al. (1991) Modulation of mouse complement receptors 1 and 2 suppresses antibody responses in vivo. *J Immunol* 147(1):224–230.
31. Garcia de Vinuesa C, O'Leary P, Sze DM, Toellner KM, MacLennan IC (1999) T-independent type 2 antigens induce B cell proliferation in multiple splenic sites, but exponential growth is confined to extrafollicular foci. *Eur J Immunol* 29(4):1314–1323.
32. Toellner KM, et al. (2002) Low-level hypermutation in T cell-independent germinal centers compared with high mutation rates associated with T cell-dependent germinal centers. *J Exp Med* 195(3):383–389.
33. Lopes-Carvalho T, Foote J, Kearney JF (2005) Marginal zone B cells in lymphocyte activation and regulation. *Curr Opin Immunol* 17(3):244–250.
34. Kumar KR, et al. (2006) Regulation of B cell tolerance by the lupus susceptibility gene Ly108. *Science* 312(5780):1665–1669.
35. Roozendaal R, Carroll MC (2006) Emerging patterns in complement-mediated pathogen recognition. *Cell* 125(1):29–32.
36. Boes M, et al. (2000) Accelerated development of IgG autoantibodies and autoimmune disease in the absence of secreted IgM. *Proc Natl Acad Sci USA* 97(3):1184–1189.
37. Ehrenstein MR, Cook HT, Neuberger MS (2000) Deficiency in serum immunoglobulin (Ig)M predisposes to development of IgG autoantibodies. *J Exp Med* 191(7):1253–1258.
38. Binder CJ, Silverman GJ (2005) Natural antibodies and the autoimmunity of atherosclerosis. *Springer Seminars in Immunopathology* 26(4):385–404.

Aire controls the differentiation program of thymic epithelial cells in the medulla for the establishment of self-tolerance

Masashi Yano,[1] Noriyuki Kuroda,[1] Hongwei Han,[1] Makiko Meguro-Horike,[1] Yumiko Nishikawa,[1] Hiroshi Kiyonari,[2] Kentaro Maemura,[3] Yuchio Yanagawa,[4] Kunihiko Obata,[5] Satoru Takahashi,[6] Tomokatsu Ikawa,[7] Rumi Satoh,[7] Hiroshi Kawamoto,[7] Yasuhiro Mouri,[1] and Mitsuru Matsumoto[1]

[1]Division of Molecular Immunology, Institute for Enzyme Research, University of Tokushima, Tokushima 770-8503, Japan
[2]Laboratory for Animal Resources and Genetic Engineering, Center for Developmental Biology, Institute of Physical and Chemical Research (RIKEN) Kobe, Kobe 650-0047, Japan
[3]Department of Anatomy and Cell Biology, Division of Basic Medicine I, Osaka Medical College, Osaka, 569-8686, Japan
[4]Department of Genetic and Behavioral Neuroscience, Gunma University Graduate School of Medicine, Maebashi 371-8511, Japan
[5]Neuronal Circuit Mechanisms Research Group, RIKEN Brain Science Institute, Saitama 351-0198, Japan
[6]Institute of Basic Medical Sciences and Laboratory Animal Resource Center, Center for Tsukuba Advanced Research Alliance, University of Tsukuba, Tsukuba 305-8575, Japan
[7]Laboratory for Lymphocyte Development, RIKEN Research Center for Allergy and Immunology, Kanagawa 230-0045, Japan

The roles of autoimmune regulator (Aire) in the expression of the diverse arrays of tissue-restricted antigen (TRA) genes from thymic epithelial cells in the medulla (medullary thymic epithelial cells [mTECs]) and in organization of the thymic microenvironment are enigmatic. We approached this issue by creating a mouse strain in which the coding sequence of green fluorescent protein (GFP) was inserted into the *Aire* locus in a manner allowing concomitant disruption of functional Aire protein expression. We found that Aire$^+$ (i.e., GFP$^+$) mTECs were the major cell types responsible for the expression of Aire-dependent TRA genes such as *insulin 2* and *salivary protein 1*, whereas Aire-independent TRA genes such as *C-reactive protein* and *glutamate decarboxylase 67* were expressed from both Aire$^+$ and Aire$^-$ mTECs. Remarkably, absence of Aire from mTECs caused morphological changes together with altered distribution of mTECs committed to Aire expression. Furthermore, we found that the numbers of mTECs that express involucrin, a marker for terminal epidermal differentiation, were reduced in Aire-deficient mouse thymus, which was associated with nearly an absence of Hassall's corpuscle-like structures in the medulla. Our results suggest that Aire controls the differentiation program of mTECs, thereby organizing the global mTEC integrity that enables TRA expression from terminally differentiated mTECs in the thymic microenvironment.

CORRESPONDENCE
Mitsuru Matsumoto:
mitsuru@ier.tokushima-u.ac.jp

Abbreviations used: Ab, antibody; Ag, antigen; Aire, autoimmune regulator; APECED, autoimmune-polyendocrinopathy-candidiasis ectodermal dystrophy; CRP, C-reactive protein; EpCAM, epithelial cell adhesion molecule 1; FSC, forward scatter; GAD67, glutamate decarboxylase 67; K5, keratin 5; mTEC, medullary thymic epithelial cell; SAP1, salivary protein 1; SSC, side scatter; TRA, tissue-restricted Ag; UEA-1, *Ulex europaeus* agglutinin 1.

Autoimmune diseases are mediated by sustained adaptive immune responses specific for self-antigens (Ags) through unknown pathogenic mechanisms. Although breakdown of self-tolerance is considered to be the key event in the disease process, the mechanisms that allow the production of autoantibodies and/or autoreactive lymphocytes are largely enigmatic (1). Autoimmune-polyendocrinopathy-candidiasis ectodermal dystrophy (APECED; OMIM 240300) is a rather rare autoimmune disease affecting mainly the endocrine glands. Because mutation of a single gene, *autoimmune regulator* (*AIRE*), is solely responsible for the development of APECED, understanding the relationship between *AIRE* gene malfunction and the breakdown of self-tolerance promises to help unravel

The online version of this article contains supplemental material.

The Rockefeller University Press $30.00
J. Exp. Med. Vol. 205 No. 12 2827-2838
www.jem.org/cgi/doi/10.1084/jem.20080046

The Journal of Experimental Medicine

the pathogenesis of not only APECED but also other types of autoimmune diseases (2, 3).

One of the most important aspects of AIRE in the context of autoimmunity is its limited tissue expression in medullary thymic epithelial cells (mTEC) (4, 5). mTECs are believed to play major roles in the establishment of self-tolerance by eliminating autoreactive T cells (negative selection) and/or by producing immunoregulatory T cells, which together prevent $CD4^+$ T cell–mediated organ-specific autoimmune diseases (6, 7). For this purpose, mTECs appear to express a set of self-Ags encompassing many or most of the self-Ags expressed by parenchymal organs. Supporting this hypothesis, analysis of gene expression in the thymic stroma has demonstrated that mTECs are a specialized cell type in which promiscuous expression of a broad range of peripheral tissue-restricted Ag (TRA) genes (i.e., promiscuous gene expression) is an autonomous property (8). Aire in mTECs has been suggested to regulate this promiscuous gene expression (9–11) through as yet undetermined mechanisms.

From a mechanistic viewpoint, there are two possible models to explain the function of Aire in the thymic organogenesis required for the establishment of self-tolerance. First, Aire may play a tolerogenic role within the types of mTECs characterized by Aire expression. In other words, the presence of Aire within cells is necessary in order for them to function normally as tolerance-establishing cells. Consistent with this idea, the current prevailing view on the roles of Aire in establishing self-tolerance is that Aire-positive cells are the major cell types that show promiscuous gene expression and that the lack of Aire protein within cells impairs their tolerogenic function because of the reduced transcription of TRA genes, although the developmental process of mTECs is otherwise unaltered in the absence of Aire (model 1). The second model hypothesizes that Aire is necessary for the developmental program of mTECs, including Aire-positive cells themselves. In this case, we assume that what are called Aire-positive mTECs and other Aire-dependent cell-types do not develop normally in the absence of Aire. Given that acquisition of the properties of promiscuous gene expression depends on the maturation status of mTECs (see Results and Discussion), impaired promiscuous gene expression from Aire-deficient mice can be associated with a defect of such an Aire-dependent developmental program in mTECs (model 2). Although it is still controversial whether reduced transcription of particular TRA genes in Aire-deficient mTECs can account for the development of autoimmunity targeting the corresponding self-Ags in Aire-deficient mice by itself (11–15), it is critical to determine which model provides a more appropriate explanation of Aire-dependent promiscuous gene expression to further elucidate the molecular aspects of Aire (16). Model 1 would direct research toward the mechanisms underlying how a single *Aire* gene can regulate a large number of target genes (i.e., TRA genes), whereas model 2 would accelerate studies of the developmental program of mTECs in which Aire plays a pivotal role. These two models can be tested if we can monitor the developmental process of mTECs committed to Aire expression in both the presence and absence of functional Aire protein.

This issue regarding the roles of Aire in thymic organogenesis is also directly linked to the fundamental question of how mTECs acquire their unique ability to express a broad range of self-Ags (i.e., promiscuous gene expression). The terminal differentiation model assumes that mTECs eventually acquire the capacity for promiscuous gene expression by becoming differentiated, more mature, and more promiscuous (7, 10). This model suggests that mTECs, especially Aire-positive cells, are specialized cell types that have acquired this ability through differentiation. In this context, it is noteworthy that the transcriptional machinery necessary for promiscuous gene expression other than Aire protein is considered to be acquired by mTECs independent of Aire expression in this model. The model suggests that the transcriptional unit for promiscuous gene expression becomes fully active when Aire starts to be expressed in terminally differentiated mTECs. In contrast, the developmental model considers that promiscuous gene expression is a reflection of the multipotency of immature mTECs before the developmental fate of particular cell types is determined (17). In this model, expression of a broad spectrum of TRA genes is regulated by conserved developmental programs that are active in developing mTECs, and Aire and/or $Aire^+$ cells control this process (18). Accordingly, the developmental model considers that Aire acts at the early developmental stage of mTEC differentiation, which is in marked contrast to the timing of Aire expression proposed in the terminal differentiation model. Thus, the terminal differentiation model and the developmental model favor models 1 and 2, respectively, proposed for the roles of Aire in promiscuous gene expression and self-tolerance (19).

To investigate in more detail the roles of Aire in thymic organogenesis, we have used a knock-in mouse strategy in which the coding sequence of GFP was inserted into the *Aire* gene locus in a manner allowing concomitant disruption of functional Aire protein expression. This strategy allowed us to distinguish mTECs committed to expressing Aire from Aire-nonexpressing mTECs, in both the presence and absence of functional Aire protein. In addition, with the use of knock-in mice in which thymic TRA (i.e., *glutamate decarboxylase 67* [*GAD67*]) expression can be monitored by GFP expression we also examined the cell types of mTECs responsible for promiscuous gene expression in situ. The results suggest that Aire promotes the differentiation program of mTECs and that promiscuous gene expression is accomplished in terminally differentiated mTECs that have fully matured in the presence of Aire protein.

RESULTS

Establishment of Aire/GFP knock-in mice

To examine the molecular and cellular contribution of Aire to thymic organogenesis, we established Aire/GFP knock-in mice in which expression of the GFP gene is under the transcriptional control of the endogenous *Aire* gene. In this strategy, modification of the *Aire* gene locus was minimized by inserting a GFP-neomycin resistance (neo^r) gene cassette (gfp-neo) (20) between exon 1 and exon 2 (Fig. 1 A). After